PHYSICAL REVIEW D **86,** 023523 (2012)

# Nonminimal chaotic inflation, Peccei-Quinn phase transition, and nonthermal leptogenesis

Constantinos Pallis[1,*] and Qaisar Shafi[2,†]

[1]*Department of Physics, University of Cyprus, P.O. Box 20537, Nicosia 1678, CYPRUS*

[2]*Bartol Research Institute, Department of Physics and Astronomy, University of Delaware, Newark, Delaware 19716, USA*

(Received 1 April 2012; published 13 July 2012)

We consider a phenomenological extension of the minimal supersymmetric standard model (MSSM) which incorporates nonminimal chaotic inflation, driven by a quadratic potential in conjunction with a linear term in the frame function. Inflation is followed by a Peccei-Quinn phase transition, based on renormalizable superpotential terms, which resolves the strong *CP* and $\mu$ problems of MSSM and provide masses lower than about $10^{12}$ GeV for the right-handed (RH) (s)neutrinos. Baryogenesis occurs via nonthermal leptogenesis, realized by the out-of-equilibrium decay of the RH sneutrinos, which are produced by the inflaton's decay. Confronting our scenario with the current observational data on the inflationary observables, the light-neutrino masses, the baryon asymmetry of the universe and the gravitino limit on the reheat temperature, we constrain the strength of the gravitational coupling to rather large values ( $\sim$ 45–2950) and the Dirac neutrino masses to values between about 1 and 10 GeV.

DOI: 10.1103/PhysRevD.86.023523 PACS numbers: 98.80.Cq, 12.60.Jv

## I. INTRODUCTION

There is recently a wave of interest in implementing *nonminimal chaotic inflation* (nMCI) within both a non-*supersymmetric* (SUSY) [1–8] and a SUSY [9–13] framework. The main idea is to introduce a large nonminimal coupling of the inflaton field to the curvature scalar, $\mathcal{R}$. After that, one can make a transformation—from the *Jordan frame* (JF) to the *Einstein* (EF) one—which flattens the potential sufficiently to support nMCI. The implementation of this mechanism within *supergravity* (SUGRA) has been greatly facilitated after the developed [10] supercorformal approach to SUGRA. In particular, it is shown that the frame function can be related to a logarithmic type Kähler potential which ensures canonical kinetic terms for the scalars of the theory and incorporates an holomorphic function, $F$, which expresses the nonminimal coupling of the inflaton field to $\mathcal{R}$. Until now, the proposed models [10–13] of nMCI within SUGRA are constructed coupling quadratically the inflaton superfield with another one in the superpotential—leading thereby to a quartic potential—and adopting a quadratic term for it in $F$.

In this paper we propose a novel realization of nMCI within SUGRA, according to which the inflaton superfield is coupled linearly to another superfield in the superpotential of the model. As a consequence, a quadratic potential for the inflaton arises which supports nMCI, if the inflaton develops a linear coupling to $\mathcal{R}$. Actually, this setup represents the SUSY implementation of the model of nMCI with $n = -1$ introduced in Ref. [7]. In contrast to earlier models [10,14] which relied on the same superpotential term—see also Ref. [15]—, no extra shift symmetry is imposed on the Kälher potential. The resulting mass of the inflaton lies at the intermediate scale and the inflationary observables are principally similar to those of nMCI with quartic—not quadratic—potential and therefore, in excellent agreement with the current observational data [16].

The inflationary model can be nicely embedded in a modest phenomenological extension of the *minimal supersymmetric standard model* (MSSM) which incorporates a resolution of the strong *CP* problem [17] via a *Peccei-Quinn* (PQ) symmetry. Note that there is an increasing interest [18,19] in such models at present, since they provide us with two additional *cold dark matter* (CDM) candidates (axino and axion) beyond the lightest neutralino. In our model, a *PQ phase transition* (PQPT), tied on renormalizable [11,20] superpontential terms, can follow nMCI generating in addition, the $\mu$ term of MSSM and intermediate masses for the *right-handed* (RH) [s]neutrinos, $\nu_i^c$ [$\tilde\nu_i^c$]. As a consequence, the light-neutrino masses can be explained through the well-known seesaw mechanism [21] provided that no large hierarchies occur in the Dirac neutrino masses. The possible formation [22] of disastrous domain walls can be avoided [23,24] by introducing extra matter superfields without jeopardizing the gauge unification of MSSM. The appearance of a Lagrangian quatric coupling of the inflaton ensures its decay to $\tilde\nu_i^c$, whose the subsequent out-of-equilibrium decays can generate the *Baryon Asymmetry of the Universe* (BAU) via *nonthermal leptogenesis* (nTL) [25], consistent with the present data on neutrino data [26,27]. Our model favors mostly quasi-degenerate $\nu_i^c$—as in Ref. [28]—which enhances the contribution from the self-energy corrections to leptonic asymmetries, without jeopardizing the validity of the relevant perturbative results, though. The constraints arising from BAU and the gravitino ($\tilde G$) limit [29–31] on the reheat temperature can be met provided that the masses of $\tilde G$ lie in the multi-TeV region.

*cpallis@ucy.ac.cy
†shafi@bartol.udel.edu

 

In Sec. II we present the basic ingredients of our model, Sec. III describes the inflationary scenario, and we outline the mechanism of nTL in Sec. IV. We then restrict the model parameters in Sec. V and summarize our conclusions in Sec. VI. Throughout the text, the subscript of type, $\chi$ denotes derivation *with respect to* (w.r.t) the field $\chi$ (e.g., $\chi\chi = \partial^2/\partial\chi^2$); charge conjugation is denoted by a star and brackets are, also, used by applying disjunctive correspondence.

## II. MODEL DESCRIPTION

We focus on a PQ invariant extension of MSSM, which is augmented with (i) two superfields ($P$ and $\bar{P}$) which are necessary for the implementation of nMCI; (ii) three superfields ($S$, $\Phi$ and $\bar{\Phi}$) involved in the spontaneous breaking of the PQ symmetry, $U(1)_{\rm PQ}$; (iii) three RH neutrinos, $\nu_i^c$, which are necessitated for the realization of the seesaw mechanism; (iv) n—to be determined below—pairs of $SU(3)_{\rm C}$ triplets and antitriplets superfields, $\bar{D}_{\rm a}$ and $D_{\rm a}$ respectively, (a $= 1, \ldots,$ n) in order to avoid the formation of domain walls—c.f. Ref. [23,24]—and; (v) an equal number of pairs of $SU(2)_{\rm L}$ doublet superfields, $\bar{h}_{\rm a}$ and $h_{\rm a}$ in order to restore gauge coupling unification at one-loop—see below. Besides the superfields in the points (iv) and (v), all the others are singlets under the *Standard Model* (SM) gauge group $G_{\rm SM} = SU(3)_{\rm C} \times SU(2)_{\rm L} \times U(1)_Y$. Besides the (color) anomalous $U(1)_{\rm PQ}$, the model also possesses an anomalous $R$ symmetry $U(1)_R$ the baryon-number symmetry $U(1)_B$ and two accidental symmetries $U(1)_D$ and $U(1)_h$. The representations under $G_{\rm SM}$, and the charges under the global symmetries of the various matter and Higgs superfields are listed in Table I. Note that the lepton number is not conserved in our model.

In particular, the superpotential, $W$, of our model can be split into four parts:

$$W = W_{\rm MSSM} + W_{\rm DW} + W_{\rm CPQ} + W_{\rm NR}, \qquad (1)$$

which are analyzed in the following:

(1) $W_{\rm MSSM}$ is the part of $W$ which contains the usual terms—except for the $\mu$ term—of MSSM, supplemented by Yukawa interactions among the left-handed leptons and $\nu_i^c$:

$$W_{\rm MSSM} = h_{Dij} d_i^c Q_j H_d + h_{Uij} u_i^c Q_j H_u + h_{Eij} e_i^c L_j H_d + h_{Nij} \nu_i^c L_j H_u. \qquad (2)$$

Here, the group indices have been suppressed and summation over the generation indices $i$ and $j$ is assumed; the $i$-th generation $SU(2)_{\rm L}$ doublet left-handed quark and lepton superfields are denoted by $Q_i$ and $L_i$ respectively, and the $SU(2)_{\rm L}$ singlet antiquark [antilepton] superfields by $u_i^c$ and $d_i{}^c$ [$e_i^c$ and $\nu_i^c$] respectively. The electroweak $SU(2)_{\rm L}$ doublet Higgs superfield, which couples to the up [down] quark superfields, is denoted by $H_u$ [$H_d$].

TABLE I. Superfield Content of the Model.

| Superfields | Representations under $G_{\rm SM}$ | $R$ | PQ | $B$ | $D$ | $h$ |
|---|---|---|---|---|---|---|
| | Matter Fields | | | | | |
| $L_i$ | $(\mathbf{1}, \mathbf{2}, -1/2)$ | 0 | −1 | 0 | 0 | 0 |
| $e_i^c$ | $(\mathbf{1}, \mathbf{1}, 1)$ | 2 | −1 | 0 | 0 | 0 |
| $\nu_i^c$ | $(\mathbf{1}, \mathbf{1}, 0)$ | 2 | −1 | 0 | 0 | 0 |
| $Q_i$ | $(\mathbf{3}, \mathbf{2}, 1/6)$ | 1 | −1 | 1/3 | 0 | 0 |
| $u_i^c$ | $(\bar{\mathbf{3}}, \mathbf{1}, -2/3)$ | 1 | −1 | −1/3 | 0 | 0 |
| $d_i^c$ | $(\bar{\mathbf{3}}, \mathbf{1}, 1/3)$ | 1 | −1 | −1/3 | 0 | 0 |
| | Extra Matter Fields | | | | | |
| $D_{\rm a}$ | $(\mathbf{3}, \mathbf{1}, -1/3)$ | 1 | 1 | 0 | 1 | 0 |
| $\bar{D}_{\rm a}$ | $(\bar{\mathbf{3}}, \mathbf{1}, 1/3)$ | 1 | 1 | 0 | −1 | 0 |
| $h_{\rm a}$ | $(\mathbf{1}, \mathbf{2}, 1/2)$ | 1 | 1 | 0 | 0 | 1 |
| $\bar{h}_{\rm a}$ | $(\mathbf{1}, \mathbf{2}, -1/2)$ | 1 | 1 | 0 | 0 | −1 |
| | Higgs Fields | | | | | |
| $H_d$ | $(\mathbf{1}, \mathbf{2}, -1/2)$ | 2 | 2 | 0 | 0 | 0 |
| $H_u$ | $(\mathbf{1}, \mathbf{2}, 1/2)$ | 2 | 2 | 0 | 0 | 0 |
| $S$ | $(\mathbf{1}, \mathbf{1}, 0)$ | 4 | 0 | 0 | 0 | 0 |
| $\Phi$ | $(\mathbf{1}, \mathbf{1}, 0)$ | 0 | 2 | 0 | 0 | 0 |
| $\bar{\Phi}$ | $(\mathbf{1}, \mathbf{1}, 0)$ | 0 | −2 | 0 | 0 | 0 |
| $P$ | $(\mathbf{1}, \mathbf{1}, 0)$ | 6 | 1 | 0 | 0 | 0 |
| $\bar{P}$ | $(\mathbf{1}, \mathbf{1}, 0)$ | −2 | −1 | 0 | 0 | 0 |

(2) $W_{\rm DW}$ is the part of $W$ which gives intermediate scale masses via $\langle\bar{\Phi}\rangle$—see below—to $\bar{D}_{\rm a} - D_{\rm a}$ and $\bar{h}_{\rm a} - h_{\rm a}$. Namely,

$$W_{\rm DW} = \lambda_{D{\rm a}} \bar{\Phi} \bar{D}_{\rm a} D_{\rm a} + \lambda_{h{\rm a}} \bar{\Phi} \bar{h}_{\rm a} h_{\rm a}. \qquad (3)$$

Here, we chose a basis in the $\bar{D}_{\rm a} - D_{\rm a}$ and $\bar{h}_{\rm a} - h_{\rm a}$ space where the coupling constant matrices $\lambda_{D{\rm a}}$ and $\lambda_{h{\rm a}}$ are diagonal. Although these matter fields acquire intermediate scale masses after the PQ breaking, the unification of the MSSM gauge coupling constants is not disrupted at one-loop. In fact, if we estimate the contribution of $\bar{D}_{\rm a}$, $D_{\rm a}$, and $\bar{h}_{\rm a}$ and $h_{\rm a}$ to the coefficients $b_1$, $b_2$, and $b_3$, controlling [32] the one-loop evolution of the three gauge coupling constants $g_1$, $g_2$, and $g_3$, we find that the quantities $b_2 - b_1$ and $b_3 - b_2$ (which are [32] crucial for the unification of $g_1$, $g_2$, and $g_3$) remain unaltered.

(3) $W_{\rm CPQ}$ is the part of $W$ which is relevant for nMCI, the spontaneous breaking of $U(1)_{\rm PQ}$, the decay of the inflaton and the generation of the masses of $\nu_i^c$'s and the $\mu$ term of MSSM. It takes the form

$$W_{\rm CPQ} = m\bar{P}P + \lambda_a S(\Phi\bar{\Phi} - M_{\rm PQ}^2) + \lambda_{i\nu^c} \Phi \nu_i^{c2}, \qquad (4)$$

where $M_{\rm PQ} = f_a/2$ with $f_a \simeq (10^{10}$–$10^{12})$ GeV being the axion decay constant which coincides with the PQ breaking scale. The parameters $\lambda_a$

and $f_a$ can be made positive by field redefinitions. From the terms in the *right-hand side* (RHS) of Eq. (4) we note that the imposed symmetries disallow renormalizable terms mixing $\bar{P}$ with some other superfields, which avoids undesirable instabilities faced in Ref. [11].

(4) $W_{\rm NR}$ is the part of $W$ which contains its nonrenormalizable terms. Namely, we have

$$W_{\rm NR} = \lambda_i \frac{\bar{P}S\Phi\nu_i^c}{m_{\rm P}} + \lambda_P \frac{P\bar{P}\,\bar{\Phi}\,\Phi}{m_{\rm P}} + \lambda_\mu \frac{\bar{\Phi}^2 H_u H_d}{m_{\rm P}}, \tag{5}$$

where $m_{\rm P} \simeq 2.44 \times 10^{18}$ GeV is the reduced Planck scale. The first term in the RHS of Eq. (5) helps accomplish sufficiently low reheat temperature and leads to the production of $\tilde{\nu}_i^c$'s as dictated by nTL—see Sec. IV A. Finally, the third term provides the $\mu$ term of MSSM—see below.

To get an impression for the role that each term in the RHS of Eqs. (3)–(5) play, we display the SUSY potential, $V_{\rm SUSY}$, induced from the following part of $W$

$$W_{\rm CI} = W_{\rm CPQ} + W_{\rm DW}, \tag{6}$$

which turns out to be

$$\begin{aligned} V_{\rm SUSY} = {}& m^2(|P|^2 + |\bar{P}|^2) + |\lambda_{i\nu^c}\tilde{\nu}_i^{c2} + \lambda_a S\bar{\Phi}|^2 \\ & + 4\lambda_{i\nu^c}^2|\tilde{\nu}_i^c\Phi|^2 + \lambda_a^2|\bar{\Phi}\Phi - M_{\rm PQ}^2|^2 \\ & + |\lambda_a S\Phi + \lambda_{D{\rm a}}\bar{D}_{\rm a}D_{\rm a} + \lambda_{h{\rm a}}\bar{h}_{\rm a}h_{\rm a}|^2 \\ & + \lambda_{D{\rm a}}^2(|\bar{D}_{\rm a}|^2 + |D_{\rm a}|^2)|\bar{\Phi}|^2 \\ & + \lambda_{h{\rm a}}^2(|\bar{h}_{\rm a}|^2 + |h_{\rm a}|^2)|\bar{\Phi}|^2, \end{aligned} \tag{7a}$$

where the complex scalar components of the superfields $P, \bar{P}, S, \bar{\Phi}, \Phi, \bar{D}_{\rm a}, D_{\rm a}, \bar{h}_{\rm a}$, and $h_{\rm a}$ are denoted by the same symbol as the corresponding superfields. From Eq. (6) and assuming [20] canonical Kähler potential for the hidden sector fields, we can also derive the soft SUSY-breaking part of the inflationary potential which reads:

$$\begin{aligned} V_{\rm soft} = {}& m_{\phi^\alpha}^2\phi^\alpha\phi_\alpha^* + (mBP\bar{P} - {\rm a}_{\rm T}\lambda_a S M_{\rm PQ}^2 \\ & + \lambda_{D{\rm a}}A_{D{\rm a}}\bar{\Phi}\bar{D}_{\rm a}D_{\rm a} + \lambda_{h{\rm a}}A_{h{\rm a}}\bar{\Phi}\bar{h}_{\rm a}h_{\rm a} + \lambda_a A_a S\Phi\bar{\Phi} \\ & + \lambda_{i\nu^c}A_{i\nu^c}\Phi\nu_i^c + {\rm H.c.}) \end{aligned} \tag{7b}$$

where $m_{\phi^\alpha}$, with

$$\phi^\alpha = P, \bar{P}, S, \bar{\Phi}, \Phi, \tilde{\nu}_i^c, \bar{D}_{k{\rm a}}, D_{k{\rm a}}, \bar{h}_{l{\rm a}}, h_{l{\rm a}} \tag{8}$$

$A_a$, $A_{i\nu^c}$, $A_{D{\rm a}}$, $A_{h{\rm a}}$, $B$ and ${\rm a}_{\rm T}$ are soft SUSY-breaking mass parameters of order 1 TeV. From the potential in Eqs. (7a) and (7b), we find that the SUSY vacuum lies at

$$\langle P\rangle = \langle\bar{P}\rangle = \langle\tilde{\nu}_i^c\rangle = 0, \tag{9a}$$

$$\langle D_{k{\rm a}}\rangle = \langle\bar{D}_{k{\rm a}}\rangle = \langle h_{l{\rm a}}\rangle = \langle\bar{h}_{l{\rm a}}\rangle = 0, \tag{9b}$$

and

$$\langle S\rangle = \frac{|A_a| + |{\rm a}_{\rm T}|}{2\lambda_a}, \qquad |\langle\phi_\Phi\rangle| = 2|\langle\Phi\rangle| = 2|\langle\bar{\Phi}\rangle| = f_a, \tag{9c}$$

where the resulting $\langle S\rangle$ is of the order of TeV—cf. Ref. [20]—and we have introduced the canonically normalized scalar field $\phi_\Phi = 2\Phi = 2\bar{\Phi}$. Also, we use the subscripts $k = 1, 2, 3$ and $l = 1, 2$ to denote the components of $D_{\rm a}$, $\bar{D}_{\rm a}$ and $h_{\rm a}$, $\bar{h}_{\rm a}$, respectively. Note that, since the sum of the arguments of $\langle\bar{\Phi}\rangle$, $\langle\Phi\rangle$ must be 0, $\bar{\Phi}$ and $\Phi$ can be brought to the real axis by an appropriate PQ transformation. After the spontaneous breaking of $U(1)_{\rm PQ}$, the third term in Eq. (4) generates intermediate scale masses, $M_{i\nu^c}$ for the $\nu_i^c$'s and, thus, seesaw masses [21] for the light neutrinos—see Sec. IV. The third term in the RHS of Eq. (5) leads to the $\mu$ term of MSSM, with $|\mu| \sim \lambda_\mu|\langle\bar{\Phi}\rangle|^2/m_{\rm P}$, which is of the right magnitude if $|\langle\bar{\Phi}\rangle| = f_a/2 \simeq 5 \times 10^{11}$ GeV, $\lambda_\mu \sim (0.001\text{–}0.01)$. Finally, since $\langle\bar{\Phi}\Phi\rangle/m_{\rm P} = M_{\rm PQ}^2/m_{\rm P} \ll m \simeq 10^{16}$ GeV—see Sec. III B and V B 1—the second term in the RHS of Eq. (5) has no impact on our results.

Nonetheless, $W_{\rm CI}$ also gives rise to a stage of nMCI within SUGRA, if it is combined with a suitable Kähler potential, $K$, related to the frame function, $\Omega_{\rm CI}$ via

$$K = -3m_{\rm P}^2\ln(-\Omega_{\rm CI}/3). \tag{10}$$

In JF a specific form of $\Omega_{\rm CI}$'s—see Ref. [10,11]—ensures canonical kinetic terms of the fields involved and a nonminimal coupling of the inflaton to $\mathcal{R}$ represented by an holomorphic function $F(P)$. Going from JF to EF, and expanding the EF potential, $\hat{V}$, along a stable direction—usually with all the fields besides inflaton placed at the origin—$\hat{V}$ takes the simple form

$$\hat{V}_{\rm CI0} \simeq V_{\rm SUSY}/f(\sigma)^2, \tag{11}$$

where $\sigma = \sqrt{2}|P|$ and $f$ can be found expanding $\Omega_{\rm CI}$. Vanishing of the noninflaton fields ensures, also, the elimination of some extra kinetic terms for scalars from the auxiliary vector fields—see Ref. [9–11].

Let us emphasize here that the coupling of $P$ to $\bar{P}$ is crucial in order to obtain the simple form of $\hat{V}_{\rm CI0}$ in Eq. (11), since only terms including derivatives of $W_{\rm CI}$ w.r.t $\bar{P}$ survive in the EF SUGRA potential—see Sec. III A. This fact ensures the appearance of just one dominant power of $\sigma$ in the numerator of the SUGRA scalar potential. Such a construction is not possible, e.g., for a superpotential term of the form $mP^2$. Applying the strategy, described above Eq. (11) in our case, we can observe that along the direction

$$\theta = \bar{P} = S = \bar{\Phi} = \Phi = \tilde{\nu}_i^c = \bar{D}_{k{\rm a}} = D_{k{\rm a}} = \bar{h}_{l{\rm a}} = h_{l{\rm a}} = 0, \tag{12a}$$

with $\theta = {\rm arg}P$, $V_{\rm SUSY}$ in Eq. (7a) becomes

$$V_{\rm SUSY} = \frac{1}{2}m^2\sigma^2 + \lambda_a^2 M_{\rm PQ}^4. \quad (12b)$$

Clearly, for $\sigma \gg f_a$, $V_{\rm SUSY}$ tends to a quadratic potential which can be flattened, according to Eq. (11), if $f$ is mainly proportional to $\sigma$, i.e., if $F$ is a linear function of $P$ with a sizable coupling constant $c_{\mathcal{R}}$. Therefore, we are led to adopt the following frame function:

$$\Omega_{\rm CI} = -3 + \frac{\phi^\alpha\phi^*_\alpha}{m_{\rm P}^2} - \frac{k_{\bar P}}{m_{\rm P}^4}|\bar P|^4 - (F(P) + F^*(P^*)), \quad (13a)$$

with $\phi^\alpha$'s defined in Eq. (8) and the nonminimal gravitational coupling

$$F = 3c_{\mathcal{R}}P/\sqrt{2}m_{\rm P}, \quad (13b)$$

which breaks explicitly the imposed $R$ and PQ symmetries during nMCI. In Eq. (13a) the coefficients $k_{\bar P}$ and $c_{\mathcal{R}}$, for simplicity, are taken real. We remark that we add the third term in the RHS of Eq. (13a) to cure the tachyonic mass problem encountered in similar models [9,10]—see Sec. III A.

For $P \ll m_{\rm P}$, we can show—see Sec. IV A—that an instability occurs in the PQ system which can drive a PQPT which leads to the v.e.vs in Eq. (9c). Also, at the SUSY vacuum the explicit breaking of $U(1)_R \times U(1)_{\rm PQ}$ through Eq. (13b) switches off—see Eq. (9a). A closer look, however, reveals that instanton and soft SUSY-breaking effects explicitly break $U(1)_R \times U(1)_{\rm PQ}$ to $\mathbb{Z}_2 \times \mathbb{Z}_{2({\rm n}-6)}$, as can be deduced from the solutions of the system

$$4r = 0\,({\rm mod}\,2\pi) \text{ and } 2({\rm n}-6)p - 12r = 0\,({\rm mod}\,2\pi), \quad (14)$$

where $r$ and $p$ are the phases of a $U(1)_R$ and $U(1)_{\rm PQ}$ rotation respectively. Here, we take into account that the $R$ charge of $W$ and, thus, of all the soft SUSY-breaking term is 4 and that the sum of the $R$ [PQ] charges of the $SU(3)_{\rm C}$ triplets and antitriplets is $-12$ [$2({\rm n}-6)$]. Note that no loop-induced PQ-violating term—as this appearing in the first paper of Ref. [13]—is detected in our case. It is then important to ensure that $\mathbb{Z}_2 \times \mathbb{Z}_{2({\rm n}-6)}$ is not spontaneously broken by $\langle\Phi\rangle$ and $\langle\bar\Phi\rangle$, since otherwise cosmologically disastrous domain walls are produced [22] during PQPT. This goal can be accomplished by adjusting conveniently the number $n$ of $\bar D_{\rm a} - D_{\rm a}$ and $\bar h_{\rm a} - h_{\rm a}$—see Table I. Indeed, when ${\rm n} = 5$ or $7$ we obtain $2p = 0({\rm mod}\,2\pi)$ and therefore, $\mathbb{Z}_2 \times \mathbb{Z}_{2({\rm n}-6)}$ is not spontaneously broken by $\langle\Phi\rangle$ and $\langle\bar\Phi\rangle$. The residual unbroken $\mathbb{Z}_2$ subgroup of $U(1)_{\rm PQ}$ can be identified with the usual matter parity of MSSM—see Table I—which prevents the rapid proton decay and ensures the stability of the *lightest SUSY particle* (LSP).

## III. THE INFLATIONARY EPOCH

In Sec. III A we describe the salient features of our inflationary model and in Sec. III B we extract the inflationary observables.

### A. Structure of the inflationary potential

The EF F–term (tree level) SUGRA scalar potential, $\hat V_{\rm CI0}$, of our model is obtained from $W_{\rm CI}$ in Eq. (6) and $K$ in Eqs. (10) and (13a) by applying [9]

$$\hat V_{\rm CI0} = e^{K/m_{\rm P}^2}\left(K^{\alpha\bar\beta}{\rm F}_\alpha {\rm F}_{\bar\beta} - 3\frac{|W_{\rm CI}|^2}{m_{\rm P}^2}\right), \quad (15a)$$

with

$$K_{\alpha\bar\beta} = K_{,\phi^\alpha\phi^{*\bar\beta}}, \qquad K^{\bar\beta\alpha}K_{\alpha\bar\gamma} = \delta^{\bar\beta}_{\bar\gamma} \quad (15b)$$

and

$${\rm F}_\alpha = W_{{\rm CI},\phi^\alpha} + K_{,\phi^\alpha}W_{\rm CI}/m_{\rm P}^2, \quad (15c)$$

where the $\phi^\alpha$'s are given in Eq. (8). From the resulting $\hat V_{\rm CI0}$, we can deduce that along the field directions in Eq. (12a),

$$\hat V_{\rm CI0} = \frac{m^2 m_{\rm P}^2 x_\sigma^2 + 4\lambda_a^2 M_{\rm PQ}^4/m_{\rm P}^4}{2f^2} \simeq \frac{m^2 m_{\rm P}^2 x_\sigma^2}{2f^2}, \quad (16a)$$

where $x_\sigma = \sigma/m_{\rm P}$ and, according to the general recipe [9–11], the function

$$f = 1 + c_{\mathcal{R}}x_\sigma - x_\sigma^2/6 \quad (16b)$$

expresses the nonminimal coupling of $\sigma$ to $\mathcal{R}$ in JF. From Eq. (16a), we can verify that for $c_{\mathcal{R}} \gg 1$ and $x_\sigma \ll \sqrt{6}$, $\hat V_{\rm CI}$ develops a plateau since $M_{\rm PQ} \ll m_{\rm P}$—see Sec. III B. Along the trajectory in Eq. (12a), we can estimate the constant potential energy density

$$\hat V_{\rm CI0} = \frac{m^2\sigma^2}{2f^2} \simeq \frac{m^2 m_{\rm P}^2}{2c_{\mathcal{R}}^2}, \quad (17a)$$

and the corresponding Hubble parameter

$$\hat H_{\rm CI} = \frac{\hat V_{\rm CI0}^{1/2}}{\sqrt{3}m_{\rm P}} \simeq \frac{m}{\sqrt{6}c_{\mathcal{R}}}. \quad (17b)$$

In order to check the stability of the direction in Eq. (12a) w.r.t the fluctuations of the various fields, we expand them in real and imaginary parts according to the prescription

$$P = \frac{\sigma e^{i\theta}}{\sqrt{2}} \quad \text{and} \quad X = \frac{\chi_1 + i\chi_2}{\sqrt{2}}, \quad (18a)$$

where

$$X = \bar P, S, \bar\Phi, \Phi, \tilde\nu_i^c, \bar D_{ka}, D_{ka}, \bar h_{la}, h_{la} \quad (18b)$$

and

TABLE II. The mass spectrum of the model during nMCI.

| Fields | Eingestates | Mass-Squared |
|---|---|---|
| | Bosons | |
| 1 real scalar | $\hat{\theta}$ | $c_{\mathcal{R}} m^2 x_\sigma / f^3 J^2 \simeq 4H_{\rm CI}^2$ |
| 2 real scalars | $\hat{\bar{p}}_1,\ \hat{\bar{p}}_2$ | $m^2(2k_{\bar{p}} c_{\mathcal{R}} x_\sigma^3 + (-c_{\mathcal{R}} x_\sigma + (6k_{\bar{p}} - 1)c_{\mathcal{R}}^2 x_\sigma^2)/2J^2 f^2)/f^2$ |
| 2 real scalars | $\hat{s}_1,\ \hat{s}_2$ | $(2\lambda_a M_{\rm PQ}^4/m_{\rm P}^2 + m^2 x_\sigma^2)/3f^2$ |
| 6 real scalars | $\hat{\nu}_{1i},\ \hat{\nu}_{2i}$ | $(2\lambda_a M_{\rm PQ}^4/m_{\rm P}^2 + m^2 x_\sigma^2)/f^2$ |
| 4 real scalars | $\frac{\hat{\bar{\phi}}_1 \pm \hat{\phi}_1}{\sqrt{2}},\ \frac{\hat{\bar{\phi}}_2 \pm \hat{\phi}_2}{\sqrt{2}}$ | $(m^2 x_\sigma^2/3 \pm \lambda_a^2 M_{\rm PQ}^2 f)/f^2$ |
| 6n real scalars | $\hat{D}_{1ka},\ \hat{D}_{2ka}$ | $(2\lambda_a M_{\rm PQ}^4/m_{\rm P}^2 + m^2 x_\sigma^2)/f^2$ |
| 6n real scalars | $\hat{\bar{D}}_{1ka},\ \hat{\bar{D}}_{2ka}$ | $(2\lambda_a M_{\rm PQ}^4/m_{\rm P}^2 + m^2 x_\sigma^2)/f^2$ |
| 4n real scalars | $\hat{h}_{1la},\ \hat{h}_{2la}$ | $(2\lambda_a M_{\rm PQ}^4/m_{\rm P}^2 + m^2 x_\sigma^2)/f^2$ |
| 4n real scalars | $\hat{\bar{h}}_{1la},\ \hat{\bar{h}}_{2la}$ | $(2\lambda_a M_{\rm PQ}^4/m_{\rm P}^2 + m^2 x_\sigma^2)/f^2$ |
| | Fermions | |
| 2 Weyl spinors | $\frac{\hat{\psi}_{\bar{P}} \pm \hat{\psi}_P}{\sqrt{2}}$ | $m^2(6 + x_\sigma^2)^2/36f^2$ |

$$\chi = \bar{p},\, s,\, \bar{\phi},\, \phi,\, \nu_i,\, \bar{D}_{ka},\, D_{ka},\, \bar{h}_{la},\, h_{la}, \tag{18c}$$

respectively. Along the trajectory in Eq. (12a) we find

$$(K_{\alpha\bar{\beta}}) = \mathrm{diag}\Big(J^2, \underbrace{1/f, \ldots, 1/f}_{7+10\mathrm{n\ elements}}\Big), \tag{19a}$$

where

$$J = \sqrt{\frac{1}{f} + \frac{3}{2} m_{\rm P}^2 \left(\frac{f_{,\sigma}}{f}\right)^2} = \frac{\sqrt{2 + 3c_{\mathcal{R}}^2}}{\sqrt{2} f} \simeq \sqrt{\frac{3}{2}} \frac{1}{x_\sigma}\cdot \tag{19b}$$

Consequently, we can introduce the EF canonically normalized fields, $\hat{\sigma}$, $\hat{\theta}$ and $\hat{\chi}$, as follows—cf. Ref. [9–12]:

$$K_{\alpha\bar{\beta}} \dot{\phi}^\alpha \dot{\phi}^{*\bar{\beta}} = \frac{1}{2}(\dot{\hat{\sigma}}^2 + \dot{\hat{\theta}}^2) + \frac{1}{2} \sum_\chi (\dot{\hat{\chi}}_1^2 + \dot{\hat{\chi}}_2^2), \tag{20}$$

where the dot denotes derivation w.r.t the JF cosmic time, $t$ and the hatted fields are defined as follows

$$\frac{d\hat{\sigma}}{d\sigma} = J, \qquad \hat{\theta} \simeq J\sigma\theta \quad \text{and} \quad \hat{\chi} \simeq \frac{\chi}{\sqrt{f}}\cdot \tag{21}$$

Note that $\dot{\hat{\theta}} \simeq J\sigma\dot{\theta}$ since $J\sigma \simeq \sqrt{3/2} m_{\rm P}$—see Eq. (19b). On the other hand, we can show that during a stage of slow-roll nMCI, $\dot{\hat{\chi}} \simeq \dot{\chi}/\sqrt{f}$ since the quantity $\dot{f}/2f^{3/2}\chi$, involved in relating $\dot{\hat{\chi}}$ to $\dot{\chi}$, turns out to be negligibly small compared with $\dot{\hat{\chi}}$. Indeed, the $\hat{\chi}$'s acquire effective masses $m_{\hat{\chi}} \gg \hat{H}_{\rm CI}$—see below—and therefore enter a phase of oscillations about $\hat{\chi} = 0$ with reducing amplitude. Neglecting the oscillating part of the relevant solutions, we find

$$\chi \simeq \hat{\chi}_0 \sqrt{f} e^{-2\hat{N}/3} \quad \text{and} \quad \dot{\hat{\chi}} \simeq -2\chi_0 \sqrt{f} \hat{H}_{\rm CI} \hat{\eta}_\chi e^{-2\hat{N}/3}, \tag{22}$$

where $\hat{\chi}_0$ represents the initial amplitude of the oscillations, $\hat{\eta}_\chi = m_{\hat{\chi}}^2/3\hat{H}_{\rm CI}$ and we assume $\dot{\hat{\chi}}(t = 0) = 0$. Taking into account the approximate expressions for $\dot{\sigma}$ and the slow-roll parameter $\hat{\epsilon}$, which are displayed in Sec. III B, we find

$$-\frac{\dot{f}}{2f^{3/2}}\chi = \frac{c_{\mathcal{R}} \hat{\epsilon} \hat{H}_{\rm CI}^2}{m_{\hat{\chi}}^2} \dot{\hat{\chi}} \ll \dot{\hat{\chi}}. \tag{23}$$

The masses that the various scalars acquire during nMCI are presented in Table II. To this end, we expand $\hat{V}_{\rm CI0}$ in Eq. (15a) to quadratic order in the fluctuations around the direction of Eq. (12a). As we observe from the relevant eigenvalues of the mass-squared matrices, no instability—as the one found in Ref. [11]—arises in the spectrum. In particular, it is evident that $k_{\bar{p}} \gtrsim 1$ assists us to achieve positivity of the mass-squared associated with the scalars $\hat{\bar{p}}_{1,2}$, $m_{\hat{\bar{p}}}^2$—in accordance with the results of Ref. [9,10]. It is remarkable that mass-squared corresponding to $\tilde{\nu}_i^c$, $D_{ka}$, $\bar{D}_{ka}$, $h_{la}$, $\bar{h}_{la}$ are independent of the relevant superpotential couplings $\lambda_{i\nu^c}$, $\lambda_{Da}$ and $\lambda_{ha}$. We have also numerically verified that the various masses remain greater than $\hat{H}_{\rm CI}$ during the last 50–60 e-foldings of nMCI, and so any inflationary perturbations of the fields other than the inflaton are safely eliminated.

In Table II we also present the masses squared of chiral fermions of the model along the direction of Eq. (12a). Inserting these masses into the well-known Coleman-Weinberg formula [33], we can find the one-loop radiative corrections, $V_{\rm rc}$, in our model which can be written as

$$V_{\rm rc} = \frac{1}{64\pi^2}\bigg(m_{\hat\theta}^4 \ln\frac{m^2_{\hat p}}{\Lambda^2} + 2m_{\hat{\bar p}}^4 \ln\frac{m^2_{\hat{\bar p}}}{\Lambda^2} + 2m_{\hat s}^4 \ln\frac{m^2_{\hat s}}{\Lambda^2} + 6m_{\hat\nu}^4 \ln\frac{m^2_{\hat\nu}}{\Lambda^2} + 2m_{\hat\phi_+}^4 \ln\frac{m^2_{\hat\phi_+}}{\Lambda^2} + 2m_{\hat\phi_-}^4 \ln\frac{m^2_{\hat\phi_-}}{\Lambda^2} + 20{\rm n}m_{\hat D}^4 \ln\frac{m^2_{\hat D}}{\Lambda^2} - 4m_{\hat\psi_\pm}^4 \ln\frac{m^2_{\hat\psi_\pm}}{\Lambda^2}\bigg), \tag{24}$$

where $\Lambda = m_{\rm P}/c_{\mathcal R}$ is the cutoff scale of the effective theory—see Sec. V A—and the involved above masses squared $m^2_{\hat\theta}$, $m^2_{\hat p}$, $m^2_{\hat s}$, $m^2_{\hat\nu}$, $m^2_{\hat\phi_\pm}$, $m^2_{\hat D}$ and $m^2_{\hat\psi_\pm}$ are equal to the ones listed in the third column of Table II from top to the bottom. Note that the masses squared of all the extra matter fields are equal to $m^2_{\hat D}$. Based on the one-loop corrected EF potential

$$\hat V_{\rm CI} = \hat V_{\rm CI0} + V_{\rm rc}, \tag{25}$$

we can proceed to the analysis of nMCI in EF, employing the standard slow-roll approximation [34]. It can be shown [35] that the results calculated this way are the same as if we had calculated them using the nonminimally coupled scalar field in JF. As expected and verified numerically, $V_{\rm rc}$ does not affect the inflationary dynamics and predictions, in the major part of the allowed parameter space—see Sec. V B 1—since the inflationary path already possesses a slope at the classical level—see below.

### B. The inflationary observables

According to our analysis above, the universe undergoes a period of slow-roll nMCI, which is determined by the condition—see e.g. Ref. [34]:

$$\max\{\hat\epsilon(\sigma), |\hat\eta(\sigma)|\} \le 1,$$

where

$$\hat\epsilon = \frac{m_{\rm P}^2}{2}\left(\frac{\hat V_{{\rm CI},\hat\sigma}}{\hat V_{\rm CI}}\right)^2 = \frac{m_{\rm P}^2}{2J^2}\left(\frac{\hat V_{{\rm CI},\sigma}}{\hat V_{\rm CI}}\right)^2 \simeq \frac{4m_{\rm P}^2}{3c_{\mathcal R}^2\sigma^2}, \tag{26a}$$

and

$$\hat\eta = m_{\rm P}^2\frac{\hat V_{{\rm CI},\hat\sigma\hat\sigma}}{\hat V_{\rm CI}} = \frac{m_{\rm P}^2}{J^2}\left(\frac{\hat V_{{\rm CI},\sigma\sigma}}{\hat V_{\rm CI}} - \frac{\hat V_{{\rm CI},\sigma}}{\hat V_{\rm CI}}\frac{J_{,\sigma}}{J}\right) \simeq -4m_{\rm P}/3c_{\mathcal R}\sigma. \tag{26b}$$

Here, we employ Eqs. (17a) and (19b) and the following approximate relations:

$$\hat V_{{\rm CI},\sigma} \simeq \frac{m^2 m_{\rm P}}{c_{\mathcal R}^3 x_\sigma^2} \quad \text{and} \quad \hat V_{{\rm CI},\sigma\sigma} \simeq -\frac{2m^2}{c_{\mathcal R}^3 x_\sigma^3}. \tag{27}$$

The numerical computation reveals that nMCI terminates due to the violation of the $\hat\epsilon$ criterion at $\sigma = \sigma_{\rm f}$, which is calculated to be

$$\hat\epsilon(\sigma_{\rm f}) = 1 \Rightarrow \sigma_{\rm f} = \frac{2}{\sqrt3}\frac{m_{\rm P}}{c_{\mathcal R}}. \tag{28}$$

We note, in passing, that for $\sigma \ge \sigma_{\rm f}$ the evolution of $\hat\sigma$—or $\sigma$ via Eq. (19b)—is governed by the equation of motion

$$3\hat H_{\rm CI}\frac{d\hat\sigma}{d\hat t} = -\hat V_{{\rm CI},\hat\sigma} \Rightarrow \dot\sigma = -\frac{2\sqrt2 m}{3\sqrt3}\sqrt{\frac{m_{\rm P}^3}{c_{\mathcal R}^3\sigma}}, \tag{29}$$

where $\hat t$ is the EF cosmic time with $d\hat t = \sqrt{f}dt$. Using Eqs. (26a) and (29), we can derive Eq. (23).

The number of e-foldings, $\hat N_*$, that the scale $k_* = 0.002/{\rm Mpc}$ suffers during nMCI can be calculated through the relation

$$\hat N_* = \frac{1}{m_{\rm P}^2}\int_{\hat\sigma_{\rm f}}^{\hat\sigma_*} d\hat\sigma\frac{\hat V_{\rm CI}}{\hat V_{{\rm CI},\hat\sigma}} = \frac{1}{m_{\rm P}^2}\int_{\sigma_{\rm f}}^{\sigma_*} d\sigma J^2\frac{\hat V_{\rm CI}}{\hat V_{{\rm CI},\sigma}}, \tag{30}$$

where $\sigma_*[\hat\sigma_*]$ is the value of $\sigma[\hat\sigma]$ when $k_*$ crosses the inflationary horizon. Given that $\sigma_{\rm f} \ll \sigma_*$, we can write $\sigma_*$ as a function of $\hat N_*$ as follows

$$\hat N_* \simeq \frac{3c_{\mathcal R}}{4m_{\rm P}}(\sigma_* - \sigma_{\rm f}) \Rightarrow \sigma_* \simeq \frac{4\hat N_*}{3c_{\mathcal R}}m_{\rm P}. \tag{31}$$

The power spectrum $P_{\mathcal R}$ of the curvature perturbations generated by $\sigma$ at the pivot scale $k_*$ is estimated as follows

$$P_{\mathcal R}^{1/2} = \frac{1}{2\pi m_{\rm P}^2}\sqrt{\frac{\hat V_{\rm CI}(\sigma_*)}{6\hat\epsilon(\sigma_*)}} \simeq \frac{m\hat N_*}{6\pi m_{\rm P}c_{\mathcal R}}, \tag{32}$$

where Eq. (31) is employed to derive the last equality of the relation above. Since the scalars listed in Table II are massive enough during nMCI, $P_{\mathcal R}^{1/2}$ can be identified with its central observational value—see Sec. V—with almost constant $\hat N_*$. The resulting relation reveals that $m$ is to be proportional to $c_{\mathcal R}$. Indeed we find

$$m = 6\pi m_{\rm P}c_{\mathcal R}P_{\mathcal R}^{1/2}/\hat N_* \Rightarrow m = 4.1\times10^{13}c_{\mathcal R}\ {\rm GeV}, \tag{33}$$

for $\hat N_* \simeq 55$. At the same pivot scale, we can also calculate the (scalar) spectral index, $n_{\rm s}$, its running, $a_{\rm s}$, and the scalar-to-tensor ratio, $r$, via the relations:

$$n_{\rm s} = 1 - 6\hat\epsilon_* + 2\hat\eta_* \simeq 1 - 2/\hat N_*, \tag{34a}$$

$$\alpha_{\rm s} = \frac{2}{3}(4\hat\eta_*^2 - (n_{\rm s}-1)^2) - 2\hat\xi_* \simeq -2/\hat N_*^2, \tag{34b}$$

$$r = 16\hat\epsilon_* \simeq 12/\hat N_*^2, \tag{34c}$$

where $\hat\xi = m_{\rm P}^4\hat V_{{\rm CI},\hat\sigma}\hat V_{{\rm CI},\hat\sigma\hat\sigma\hat\sigma}/\hat V_{\rm CI}^2 = m_{\rm P}\sqrt{2\hat\epsilon}\hat\eta_{,\sigma}/J + 2\hat\eta\hat\epsilon$ and the variables with subscript $*$ are evaluated at $\sigma = \sigma_*$. Comparing the results of this section with the observationally favored values [16], we constrain the parameters of our model in Sec. V B 1.

## IV. NON-THERMAL LEPTOGENESIS

A complete SUSY inflationary scenario should specify the transition to the radiation dominated era and also explain the origin of the observed BAU consistently with the $\tilde{G}$ constraint. These goals can be accomplished within our setup, as we describe in this section. Namely, the basic features of the post-inflationary evolution are exhibited in Sec. IV A and the topic of nTL in conjunction with the present neutrino data is analyzed in Sec. IV B.

### A. The general setup

When nMCI is over, the inflaton continues to roll down towards the SUSY vacuum, Eqs. (9a)–(9c). Note that when $x_\sigma \lesssim \sqrt{3}\lambda_a M_{\rm PQ}/m$, one scalar originating from the superfields $\Phi$ and $\bar\Phi$—see Table I—acquires a negative mass-squared triggering thereby the PQPT. As the inflaton continues its rolling, there is a brief stage of tachyonic preheating [36] which does not lead to significant particle production [37]. Soon afterwards, it settles into a phase of damped oscillations about the minimum of the $\hat{V}_{\rm CI0}$. Since no gauge symmetry is broken during nMCI, no superheavy bosons are produced and therefore no particle production via the mechanism of instant preheating [38] occurs. Also, since the inflaton cannot decay via renormalizable interactions to SM particles, effects of narrow parametric resonance [36] are also absent in our regime.

Nonetheless, the standard perturbative approach to the inflaton decay provides a very efficient decay rate. Namely, at the SUSY vacuum the fields involved acquire the v.e.vs shown in Eqs. (9a)–(9c) giving rise to the mass spectrum presented in Table III. There we can show the mass, $m_{\rm I}$, of the (canonically normalized) inflaton $\hat{P}$ and the masses $M_{i\nu^c}$ of the RH [s]neutrinos, $\nu_i^c$ [$\tilde\nu_i^c$], which play a crucial role in our scenario of nTL. Note that since $\langle\Phi\rangle = \langle\bar\Phi\rangle = M_{\rm PQ} \ll m_{\rm P}$, $\langle\Omega\rangle \simeq -3$ and so $\langle f\rangle \simeq 1$. Therefore, apart from $\hat{P}$, the EF canonically normalized field are not distinguished from the JF ones at the SUSY vacuum. On the other hand, $\hat{P}$ can be expressed as a function of $P$ through the relation

$$\frac{\hat{P}}{P} = \langle J\rangle \quad \text{where } \langle J\rangle = \sqrt{1 + 3c_{\mathcal{R}}^2/2}. \tag{35}$$

TABLE III. The mass spectrum of the model at the SUSY vacuum.

| Eigenstates: Scalars | Eigenstates: Fermions | Eigenvalues (Masses) |
|---|---|---|
| $\hat{P}$, $\bar{P}$ | $(\psi_{\bar P} \pm \psi_{\hat P})/\sqrt{2}$ | $m_{\rm I} = m/\langle J\rangle$ |
| $S$, $(\delta\bar\Phi + \delta\Phi)/\sqrt{2}$ | $(\psi_S \pm \psi_+)/\sqrt{2}$ | $m_{\rm PQ} = \sqrt{2}\lambda_a M_{\rm PQ}$ |
| $(\delta\bar\Phi - \delta\Phi)/\sqrt{2}$ | $(\psi_{\bar\Phi} - \psi_\Phi)/\sqrt{2}$ | 0 |
| $\tilde\nu_i^c$ | $\nu_i^c$ | $M_{i\nu^c} = 2\lambda_{i\nu^c} M_{\rm PQ}$ |
| $D_{ka}$, $\bar{D}_{ka}$ | $\psi_{D_{ka}}$, $\psi_{\bar{D}_{ka}}$ | $m_{D_a} = \lambda_{D_a} M_{\rm PQ}$ |
| $h_{la}$, $\bar{h}_{la}$ | $\psi_{h_{la}}$, $\psi_{\bar{h}_{la}}$ | $m_{h_a} = \lambda_{h_a} M_{\rm PQ}$ |

Making use of Eq. (33) we can infer that $m_{\rm I}$ is kept independent of $c_{\mathcal{R}}$ and almost constant at the level of $10^{13}$ GeV. Indeed,

$$m_{\rm I} \simeq \frac{m}{\langle J\rangle} = \sqrt{\frac{2}{3}}\frac{m}{c_{\mathcal{R}}} \simeq 2\sqrt{3}\pi m_{\rm P}\frac{P_{\mathcal{R}}^{1/2}}{\hat{N}} \simeq 10^{13}\ \text{GeV}, \tag{36}$$

where the WMAP7 value of $P_{\mathcal{R}}^{1/2}$—see Sec. VA—is employed in the last step of the relation above. In the expressions of the various eigenstates listed in Table III, we adopt the following abbreviations

$$\delta\Phi = \Phi - M_{\rm PQ}, \qquad \delta\bar\Phi = \bar\Phi - M_{\rm PQ}, \tag{37a}$$

and

$$\psi_\pm = (\psi_{\bar\Phi} \pm \psi_\Phi)/\sqrt{2}, \tag{37b}$$

where $\psi_x$ with $x = \hat{P}, P, S, \bar\Phi, \Phi, \bar{D}_{ka}, D_{ka}, \bar{h}_{la}$, and $h_{la}$ denote the chiral fermions associated with the superfields $\hat{P}$, $P$, $S$, $\bar\Phi$, $\Phi$, $\bar{D}_{ka}$, $D_{ka}$, $h_{la}$, and $h_{la}$ respectively. The eigenstates $\psi_-$ and $\delta\Phi_-$, with

$$\delta\Phi_\pm = (\delta\bar\Phi \pm \delta\Phi)/\sqrt{2}, \tag{38}$$

contain the components of the axion supermultiplet. Namely axion [saxion] can be identified with the phase [modulus] of the complex field $\delta\Phi_-$, whereas $\psi_-$ can be interpreted as the axino. Note that the zero masses of saxion and axino can be replaced with masses of order 1 TeV if we take into account the soft SUSY-breaking masses—see discussion below Eq. (9c).

The decay of $\hat{P}$ commences when $m_{\rm I}$ becomes larger than the expansion rate and is processed via the first coupling in the RHS of Eq. (5), into $S$ and $\tilde\nu_i^c$ and $S$, $\tilde\nu_i^c$ and $\delta\Phi_+$ or $\delta\Phi_-$. The relevant Lagrangian sector is

$$\mathcal{L}_{\rm dc} = -\frac{m_{\rm I}}{m_{\rm P}}\lambda_i \hat{P}^* S\tilde\nu_i^c\left(M_{\rm PQ} + \frac{\delta\Phi_+ - \delta\Phi_-}{\sqrt{2}}\right) + \text{H.c.} \tag{39}$$

which arises from the cross term of the F-term, corresponding to $\bar{P}$, of the SUSY potential derived from the superpotential terms in Eqs. (4) and (5). Note that we have no $c_{\mathcal{R}}$-induced decay channels as in Ref. [12], since $\langle P\rangle = 0$. The interaction above gives rise to the following decay width

$$\Gamma_{\rm I} = \frac{1}{8\pi}\left(\left(\frac{M_{\rm PQ}}{m_{\rm P}}\right)^2 + \frac{1}{64\pi^2}\left(\frac{m_{\rm I}}{m_{\rm P}}\right)^2\right)m_{\rm I}\sum_{i=1}^{3}\lambda_i^2, \tag{40}$$

where we take into account that $m_{\rm I} \gg m_{\rm PQ}$ and $m_{\rm I} \gg M_{j\nu^c}$. These prerequisites are safely fulfilled when $\lambda_a$ and $\lambda_{i\nu^c}$ remain perturbative, i.e. $\lambda_a$, $\lambda_{i\nu^c} \leq \sqrt{4\pi}$—see Table III. From the two contributions to $\Gamma_{\rm I}$, the dominant one is the second one—the 3-body decay channel—originating from the two last terms of Eq. (39).

Taking also into account that the decay width of the produced $\tilde\nu_i^c$, $\Gamma_{i\nu^c}$, is much larger than $\Gamma_{\rm I}$—see below—we can infer that the reheat temperature, $T_{\rm rh}$, is exclusively determined by the $\hat{P}$ decay and is given by [39]

$$T_{\rm rh} = \left(\frac{72}{5\pi^2 g_*}\right)^{1/4}\sqrt{\Gamma_{\rm I} m_{\rm P}}, \qquad (41)$$

where $g_* \simeq 232.5$ counts the effective number of the relativistic degrees of freedom at temperature $T_{\rm rh}$ for the (s) particle spectrum of MSSM plus the particle content of the axion supermultiplet. Although the factor before the square root of Eq. (41) differs [39] slightly from other calculations of $T_{\rm rh}$—cf. Ref. [25]—the numerical result remains pretty stable and close to $10^8$ GeV—see Sec. V B 1.

If $T_{\rm rh} \ll M_{i\nu^c}$, the out-of-equilibrium condition [40] for the implementation of nTL is automatically satisfied. Subsequently, $\tilde{\nu}^c_i$ decay into $\tilde{H}_u$ and $L_i$ or $\tilde{H}^*_u$ and $\tilde{L}^*_i$ via the tree-level couplings derived from the second term of the second line of Eq. (2). Interference between tree-level and one-loop diagrams generates a lepton-number asymmetry (per $\nu^c_i$ decay) $\varepsilon_i$ [40], when $CP$ is not conserved in the Yukawa coupling constants $h_{Nij}$—see Eq. (2). The resulting lepton-number asymmetry after reheating can be partially converted through sphaleron effects into baryon-number asymmetry. However, the required $T_{\rm rh}$ must be compatible with constraints for the $\tilde{G}$ abundance, $Y_{\tilde{G}}$, at the onset of *nucleosynthesis* (BBN). In particular, the $B$ yield can be computed as

$$Y_B = -0.35\frac{5}{4}\frac{T_{\rm rh}}{m_{\rm I}}\sum_i {\rm Br}_i\varepsilon_i \ \text{ with } \ {\rm Br}_i = \frac{\lambda_i^2}{\sum_i \lambda_i^2} \qquad (42)$$

the branching ratio of $\hat{P}$ to $\tilde{\nu}^c_i$—see Eq. (40). In the formula above the first numerical factor (0.35) comes from the sphaleron effects, whereas the second one (5/4) is due to the slightly different calculation [39] of $T_{\rm rh}$—cf. Ref. [25]. On the other hand, the $\tilde{G}$ yield due to thermal production at the onset of BBN is estimated to be [31]

$$Y_{\tilde{G}} \simeq 1.9\times 10^{-22} T_{\rm rh}/{\rm GeV}. \qquad (43)$$

where we assume that $\tilde{G}$ is much heavier than the gauginos. Let us note that nonthermal $\tilde{G}$ production within SUGRA is unlikely in our scenario, since these contributions are [41] usually proportional to the v.e.v of the inflaton which is zero in our case.

Both Eqs. (42) and (43) calculate the correct values of the $B$ and $\tilde{G}$ abundances provided that no entropy production occurs for $T < T_{\rm rh}$—see also Sec. VA. This fact can be easily achieved within our setting. Indeed, following the arguments of Ref. [11], one can show that the PQ system comprised of the fields $S$ and $\delta\Phi_+$ decays via the third term in the RHS of Eq. (5) before its domination over radiation, for all relevant values of $\lambda_i$'s. Regarding the saxion, $\delta\Phi_-$, we can assume that it has mass of the order of 1 TeV, its decay mode to axions is suppressed (w.r.t the ones to gluons, Higgses and Higgsinos [19,42,43]) and the initial amplitude of its oscillations is equal to $f_a$. Under these circumstances, it can [42] decay before domination too, and evades [43] the constraints from the effective number of neutrinos for the $f_a$'s and $T_{\rm rh}$'s encountered in our model. As a consequence of its relatively large decay temperature, the LSPs produced by the saxion decay are likely to be thermalized and therefore, no upper bound on the saxion abundance is [43] to be imposed. Finally, if axino is sufficiently light it can act as a CDM candidate [18,19] with relic abundance produced predominantly thermally—due to the relatively large $T_{\rm rh}$. Otherwise, it may enhance [19] nonthermally the abundance of a Higgsino-like neutralino-LSP, rendering it a successful CDM candidate.

### B. Lepton-number asymmetry and neutrino masses

As mentioned above, the decay of $\tilde{\nu}^c_i$, emerging from the $\hat{P}$ decay, can generate a lepton asymmetry, $\varepsilon_i$, caused by the interference between the tree-level and one-loop decay diagrams, provided that a $CP$-violation occurs in $h_{Nij}$'s. The produced $\varepsilon_i$ can be expressed in terms of the Dirac mass matrix of $\nu_i$, $m_{\rm D}$, defined in a basis (called $\nu^c_i$-basis henceforth) where $\nu^c_i$ are mass eigenstates, as follows:

$$\varepsilon_i = \frac{\sum_{i\neq j}{\rm Im}[(m^\dagger_{\rm D} m_{\rm D})^2_{ij}](F_{\rm S}(x_{ij}, y_i, y_j) + F_{\rm V}(x_{ij}))}{8\pi\langle H_u\rangle^2 (m^\dagger_{\rm D} m_{\rm D})_{ii}}, \qquad (44a)$$

where we take $\langle H_u\rangle \simeq 174$ GeV, for large $\tan\beta$ and

$$x_{ij} = \frac{M_{j\nu^c}}{M_{i\nu^c}} \quad \text{and} \quad y_i = \frac{\Gamma_{i\nu^c}}{M_{i\nu^c}} = \frac{(m^\dagger_{\rm D} m_{\rm D})_{ii}}{8\pi\langle H_u\rangle^2}. \qquad (44b)$$

Also $F_{\rm V}$ and $F_{\rm S}$ represent, respectively, the contributions from vertex and self-energy diagrams which in SUSY theories read [44–46]

$$F_{\rm V}(x) = -x\ln(1+x^{-2}), \qquad (44c)$$

and

$$F_{\rm S}(x,y,z) = \frac{-2x(x^2-1)}{(x^2-1-x^2 z\ln x^2/\pi)^2 + (x^2 z - y)^2}, \qquad (44d)$$

with the latter expression written as given in Ref. [46]. When

$$\Delta_{iji} \gg 1 \quad \text{and} \quad \Delta_{ijj} \gg 1 \quad \text{with } \Delta_{ijk} = \frac{|x^2_{ij}-1|}{x_{ik} y_k}, \qquad (45)$$

(no summation is applied over the repeated indices) we can simplify $F_{\rm S}$ expanding it close to $x \simeq 1$ as follows:

$$F_{\rm S} \simeq \frac{2x}{1-x^2} \simeq \frac{1}{1-x} - \frac{1}{2}. \qquad (46)$$

The involved in Eq. (44a) $m_{\rm D}$ can be diagonalized if we define a basis—called weak basis henceforth—in which the lepton Yukawa couplings and the $SU(2)_{\rm L}$ interactions are diagonal in the space of generations. In particular we have

$$U^\dagger m_{\rm D} U^{c\dagger} = d_{\rm D} = {\rm diag}(m_{1\rm D}, m_{2\rm D}, m_{3\rm D}), \quad (47)$$

where $U$ and $U^c$ are $3\times 3$ unitary matrices which relate $L_i$ and $\nu^c_i$ (in the $\nu^c_i$-basis) with the ones $L'_i$ and $\nu^{c\prime}_i$ in the weak basis as follows:

$$L' = LU \quad \text{and} \quad \nu^{c\prime} = U^c \nu^c. \quad (48)$$

Here, we write LH lepton superfields, i.e. $SU(2)_{\rm L}$ doublet leptons, as row 3-vectors in family space and RH antilepton superfields, i.e. $SU(2)_{\rm L}$ singlet antileptons, as column 3-vectors. Consequently, the combination $m^\dagger_{\rm D} m_{\rm D}$ appeared in Eq. (44a) turns out to be a function just of $d_{\rm D}$ and $U^c$. Namely,

$$m^\dagger_{\rm D} m_{\rm D} = U^{c\dagger} d_{\rm D} d_{\rm D} U^c. \quad (49)$$

The connection of the leptogenesis scenario with the low energy neutrino data can be achieved through the seesaw formula, which gives the light-neutrino mass matrix $m_\nu$ in terms of $m_{i\rm D}$ and $M_{i\nu^c}$. Working in the $\nu^c_i$-basis, we have

$$m_\nu = -m_{\rm D} d^{-1}_{\nu^c} m^{\sf T}_{\rm D}, \quad (50)$$

where

$$d_{\nu^c} = {\rm diag}(M_{1\nu^c}, M_{2\nu^c}, M_{3\nu^c}) \quad (51)$$

with $M_{1\nu^c} \le M_{2\nu^c} \le M_{3\nu^c}$ real and positive. Solving Eq. (47) w.r.t $m_{\rm D}$ and inserting the resulting expression in Eq. (50) we extract the mass matrix

$$\bar m_\nu = U^\dagger m_\nu U^* = -d_{\rm D} U^c d^{-1}_{\nu^c} U^{c\sf T} d_{\rm D}, \quad (52)$$

which can be diagonalized by the unitary PMNS matrix satisfying

$$\bar m_\nu = U^*_\nu {\rm diag}(m_{1\nu}, m_{2\nu}, m_{3\nu}) U^\dagger_\nu \quad (53)$$

and parameterized as follows:

$$U_\nu = \begin{bmatrix} c_{12}c_{13} & s_{12}c_{13} & s_{13}e^{-i\delta} \\ U_{21\nu} & U_{22\nu} & s_{23}c_{13} \\ U_{31\nu} & U_{32\nu} & c_{23}c_{13} \end{bmatrix} \cdot \mathcal{P}. \quad (54)$$

Here

$$U_{21\nu} = -c_{23}s_{12} - s_{23}c_{12}s_{13}e^{i\delta}, \quad (55a)$$
$$U_{22\nu} = c_{23}c_{12} - s_{23}s_{12}s_{13}e^{i\delta}, \quad (55b)$$
$$U_{31\nu} = s_{23}s_{12} - c_{23}c_{12}s_{13}e^{i\delta}, \quad (55c)$$
$$U_{32\nu} = -s_{23}c_{12} - c_{23}s_{12}s_{13}e^{i\delta}, \quad (55d)$$

with $c_{ij} := \cos\theta_{ij}$, $s_{ij} := \sin\theta_{ij}$ and $\delta$ the $CP$-violating Dirac phase. The two $CP$-violating Majorana phases $\varphi_1$ and $\varphi_2$ are contained in the matrix

$$\mathcal{P} = {\rm diag}(e^{-i\varphi_1/2}, e^{-i\varphi_2/2}, 1). \quad (56)$$

Following a bottom-up approach, along the lines of Ref. [47], we can find $\bar m_\nu$ via Eq. (53) using as input parameters the low-energy neutrino observables, the $CP$ violating phases and adopting the normal or inverted hierarchical scheme of neutrino masses. Taking also $m_{i\rm D}$ as input parameters we can construct the complex symmetric matrix

$$W = -d^{-1}_{\rm D} \bar m_\nu d^{-1}_{\rm D} = U^c d_{\nu^c} U^{c\sf T} \quad (57)$$

—see Eq. (52)—from which we can extract $d_{\nu^c}$ as follows:

$$d^{-2}_{\nu^c} = U^{c\dagger} W W^\dagger U^c. \quad (58)$$

Note that $WW^\dagger$ is a $3\times 3$ complex, Hermitian matrix and can be diagonalized following the algorithm described in Ref. [48]. Having determined the elements of $U^c$ and the $M_{i\nu^c}$'s we can compute $m_{\rm D}$ through Eq. (49) and the $\varepsilon_i$'s through Eq. (44a).

## V. CONSTRAINING THE MODEL PARAMETERS

We exhibit the constraints that we impose on our cosmological setup in Sec. V A, and delineate the allowed parameter space of our model in Sec. V B.

### A. Imposed constraints

The parameters of our model can be restricted once we impose the following requirements:

(1) According to the inflationary paradigm, the horizon and flatness problems of the standard Big Bang cosmology can be successfully resolved provided that $\hat N_*$ defined by Eq. (30) takes a certain value, which depends on the details of the cosmological scenario. Employing standard methods [7], we can easily derive the required $\hat N_*$ for our model, consistent with the fact that the PQ oscillatory system remains subdominant during the post-inflationary era. Namely we obtain

$$\hat N_* \simeq 22.5 + 2\ln\frac{V_{\rm CI}(\sigma_*)^{1/4}}{1~{\rm GeV}} - \frac{4}{3}\ln\frac{V_{\rm CI}(\sigma_{\rm f})^{1/4}}{1~{\rm GeV}} + \frac{1}{3}\ln\frac{T_{\rm rh}}{1~{\rm GeV}} + \frac{1}{2}\ln\frac{f(\sigma_{\rm f})}{f(\sigma_*)}. \quad (59)$$

(2) The inflationary observables derived in Sec. III B are to be consistent with the fitting [16] of the WMAP7, BAO and $H_0$ data. As usual, we adopt the central value of $P^{1/2}_{\mathcal{R}}$, whereas we allow the remaining quantities to vary within the 95% *confidence level* (c.l.) ranges. Namely,

$$P_{\mathcal{R}}^{1/2} \simeq 4.93 \times 10^{-5}, \tag{60a}$$
$$0.944 \leq n_s \leq 0.992, \tag{60b}$$
$$-0.062 \leq \alpha_s \leq 0.018, \tag{60c}$$
$$r < 0.24. \tag{60d}$$

(3) For the realization of nMCI, we assume that $c_{\mathcal{R}}$ takes relatively large values—see e.g. Eq. (16a). This assumption may [5,49] jeopardize the validity of the classical approximation, on which the analysis of the inflationary behavior is based. To avoid this inconsistency—which is rather questionable [10,49] though—we have to check the hierarchy between the ultraviolet cutoff scale [7], $\Lambda = m_{\rm P}/c_{\mathcal{R}}$, of the effective theory and the inflationary scale, which is represented by $\hat{V}_{\rm CI}(\sigma_*)^{1/4}$ or, less restrictively, by the corresponding Hubble parameter, $\hat{H}_* = \hat{V}_{\rm CI}(\sigma_*)^{1/2}/\sqrt{3}m_{\rm P}$. In particular, the validity of the effective theory implies

$$\hat{V}_{\rm CI}(\sigma_*)^{1/4} \leq \Lambda \quad \text{or} \tag{61a}$$
$$\hat{H}_* \leq \Lambda. \tag{61b}$$

(4) To ensure that the inflaton decay according to the Lagrangian part of Eq. (39) is kinematically allowed we have to impose the constraint—see Table III:

$$m_{\rm I} \geq 2m_{\rm PQ} + M_{i\nu^c} \Rightarrow 2m_{\rm PQ} + M_{i\nu^c} \lesssim 10^{13}\ {\rm GeV}, \tag{62}$$

where we make use of Eq. (36). This requirement can be easily satisfied by constraining $\lambda_a$ and $\lambda_{i\nu^c}$ to values lower than the perturbative limit. As the inequality in Eq. (62) gets strengthened, the accuracy of Eq. (40) where masses of the decay products are neglected, increases.

(5) From the solar, atmospheric, accelerator and reactor neutrino experiments we take into account the following inputs [26]—see also Ref. [27]—on the neutrino mass-squared differences:

$$\Delta m^2_{21} = \left(7.59^{+0.2}_{-0.18}\right) \times 10^{-3}\ {\rm eV}^2, \tag{63a}$$
$$\Delta m^2_{31} = \left(2.5^{+0.09}_{-0.16}\left[-2.4^{+0.08}_{-0.09}\right]\right) \times 10^{-3}\ {\rm eV}^2, \tag{63b}$$

on the mixing angles:

$$\sin^2\theta_{12} = 0.312^{+0.017}_{-0.015}, \tag{63c}$$
$$\sin^2\theta_{13} = 0.013^{+0.007}_{-0.005}\left[0.016^{+0.008}_{-0.006}\right], \tag{63d}$$
$$\sin^2\theta_{23} = 0.52^{+0.06}_{-0.07}[0.52 \pm 0.06], \tag{63e}$$

and on the $CP$-violating Dirac phase:

$$\delta = -\left(0.61^{+0.75}_{-0.65}\left[0.41^{+0.65}_{-0.7}\right]\right)\pi \tag{63f}$$

for normal [inverted] neutrino mass hierarchy. In particular, $m_{i\nu}$'s can be determined via the relations

$$m_{2\nu} = \sqrt{m^2_{1\nu} + \Delta m^2_{21}} \tag{64a}$$

and

$$m_{3\nu} = \sqrt{m^2_{1\nu} + \Delta m^2_{31}} \tag{64b}$$

for *normally ordered* (NO) $m_{i\nu}$'s or

$$m_{1\nu} = \sqrt{m^2_{3\nu} + |\Delta m^2_{31}|} \tag{64c}$$

for *invertedly ordered* (IO) $m_{i\nu}$'s. The sum of $m_{i\nu}$'s can be bounded from above by the WMAP7 data [16]

$$\sum_i m_{i\nu} \leq 0.58\ {\rm eV} \tag{65}$$

at 95% c.l. This is more restrictive than the 95% c.l. upper bound arising from the effective electron neutrino mass in $\beta$-decay [50]:

$$m_\beta := \left|\sum_i U^2_{1i\nu} m_{i\nu}\right| \leq 2.3\ {\rm eV}. \tag{66}$$

However, in the future, the KATRIN experiment [51] expects to reach the sensitivity of $m_\beta \simeq 0.2$ eV at 90% c.l.

(6) The interpretation of BAU through nTL dictates [16] at 95% c.l.

$$Y_B = (8.74 \pm 0.42) \times 10^{-11}. \tag{67}$$

(7) In order to avoid spoiling the success of the BBN, an upper bound on $Y_{\tilde{G}}$ is to be imposed depending on the $\tilde{G}$ mass, $m_{\tilde{G}}$, and the dominant $\tilde{G}$ decay mode. For the conservative case where $\tilde{G}$ decays with a tiny hadronic branching ratio, we have [31]

$$Y_{\tilde{G}} \lesssim \begin{cases} 10^{-14} \\ 2.5\times10^{-14} \\ 4.3\times10^{-14} \\ 10^{-13} \end{cases} \text{for } m_{\tilde{G}} \simeq \begin{cases} 0.69\ {\rm TeV} \\ 5\ {\rm TeV} \\ 8\ {\rm TeV} \\ 10.6\ {\rm TeV} \end{cases}. \tag{68}$$

As we see below, this bound is achievable within our model only for $m_{\tilde{G}} \gtrsim 8$ TeV. The bound above may be somehow relaxed in the case of a stable $\tilde{G}$.

### B. Results

As can be easily seen from the relevant expressions in Secs. II and IV B, our cosmological setup depends on the following independent parameters:

$$m,\ \lambda_a,\ \lambda_\mu,\ k_{\bar{P}},\ \lambda_i,\ f_a,\ {\rm n},\ \lambda,\ m_{l\nu},\ m_{i{\rm D}},\ \varphi_1 \quad \text{and} \quad \varphi_2,$$

where $m_{l\nu}$ is the low scale mass of the lightest of $\nu_i$'s and can be identified with $m_{1\nu}[m_{3\nu}]$ for NO [IO] neutrino mass spectrum. We do not consider $c_{\mathcal{R}}$ and $\lambda_{i\nu^c}$ as independent parameters since $c_{\mathcal{R}}$ is related to $m$ via Eq. (33) while $\lambda_{i\nu^c}$ can be derived from the last six parameters above which affect exclusively the $Y_L$ calculation and can be constrained through the requirements 5 and 6 of Sec. VA. Note that the $\lambda_{i\nu^c}$'s can be replaced by $M_{i\nu^c}$'s given in Table III keeping in mind that perturbativity requires $\lambda_{i\nu^c} \leq \sqrt{4\pi}$ or $M_{i\nu^c} \leq 3.5 f_a$. Recall also that $V_{\rm rc}$ in Eq. (24) is independent of $\lambda_{Da}$, $\lambda_h \gg \lambda_a$ and depends only on n, which is set equal to 5 for definiteness. To facilitate the realization of seesaw mechanism, we take $f_a = 10^{12}$ GeV. This choice makes also possible the generation of the $\mu$ term of MSSM through the PQ symmetry breaking, since $\mu \sim 1$ TeV is obtained for $\lambda_\mu = 0.01$, whereas lower $f_a$'s dictate larger $\lambda_\mu$'s. Moreover, our computation reveals that $\varepsilon_1$ in Eq. (44a) is mostly smaller than $\varepsilon_2$ and $\varepsilon_3$. Therefore, fulfilling the baryogenesis criterion enforces us to consider $\mathsf{Br}_1 \ll \mathsf{Br}_{2,3}$ or $\lambda_1 \ll \lambda_{2,3} \sim 0.1$. Since $\varepsilon_2$ and $\varepsilon_3$ are of the same order of magnitude, the resulting $Y_B$ does not depends crucially on $\lambda_2/\lambda_3$. Therefore we believe that $\lambda_2 = \lambda_3 = 0.5$ is a representative choice—e.g., we explicitly checked that the option $\lambda_2 = 0.1$ and $\lambda_3 = 0.9$ or $\lambda_2 = 0.9$ and $\lambda_3 = 0.1$ lead to similar results. Finally, our results are independent of $\lambda_a$ and $k_{\bar{P}}$ provided Eq. (62) is fulfilled and the positivity of $m^2_{\hat{\bar{p}}}$—see Table II—is ensured, respectively. To facilitate the achievement of these objective, we get $\lambda_a = 0.01$ and $k_{\bar{P}} = 1$.

Summarizing, we set throughout our calculation:

$$k_{\bar{P}} = 1,\ \lambda_1 \leq 0.01,\ \lambda_2 = \lambda_3 = 0.5,\ \mathrm{n} = 5, \tag{69a}$$

$$\lambda_\mu = \lambda_a = 0.01 \quad \text{and} \quad f_a = 10^{12}\ \text{GeV}. \tag{69b}$$

The selected values for the above quantities give us a wide and natural allowed region for the remaining fundamental parameters of our model, as we show below concentrating separately in the inflationary period (Sec. V B 1) and in the stage of nTL (Sec. V B 2).

### *1. The stage of nonminimal inflation*

For nMCI, we use as input parameters in our numerical code $\sigma_*$, $m$ and $c_{\mathcal{R}}$. For every chosen $c_{\mathcal{R}} \gtrsim 1$ we restrict $m$ and $\sigma_*$ so that the conditions in Eq. (59)—with $T_{\rm rh}$ evaluated consistently using Eq. (41)—and (60a) are satisfied. Let us remark that, in our numerical calculations, we use the complete formulas for $\hat{V}_{\rm CI}$—see Eq. (25)—, $\hat{N}_*$, the slow-roll parameters and $P^{1/2}_{\mathcal{R}}$ in Eqs. (30), (26a), (26b), and (32) and not the approximate relations listed in Sec. III B for the sake of presentation.

Our results are displayed in Fig. 1, where we draw the allowed values of $c_{\mathcal{R}}$ (solid line) $m_{\rm I}$ (dashed line) and $T_{\rm rh}$ (dot-dashed line) [$\sigma_{\rm f}$ (solid line) and $\sigma_*$ (dashed line)] versus $m$—see Figs. 1(a) and 1(b). The constraint of Equation (61b) is satisfied along the various curves whereas Eq. (61a) is valid only along the gray and light gray segments of these. Along the light gray segments, though, we obtain $\sigma_* \gtrsim m_{\rm P}$. The lower bound on $m$ is derived from the saturation of the upper bound of inequality in Eq. (60b) whereas the upper bound comes from the fact that the enhanced resulting $m$'s destabilize the inflationary path through the radiative corrections in Eq. (25)—see Eq. (24). Indeed, $V_{\rm rc}$ starts to influence the inflationary dynamics for $m \gtrsim 1.5 \times 10^{16}$ GeV, and consequently, the variation of $\sigma_{\rm f}$ as a function of $c_{\mathcal{R}}$ or $m$—drawn in Fig. 1(b)—deviates from the behavior described in Eq. (28). On the contrary the variations of $\sigma_*$ follows Eq. (31).

In all, we obtain

$$45 \lesssim c_{\mathcal{R}} \lesssim 2950 \quad \text{and} \quad 2.5 \lesssim \frac{m}{10^{15}\ \text{GeV}} \lesssim 102 \tag{70}$$

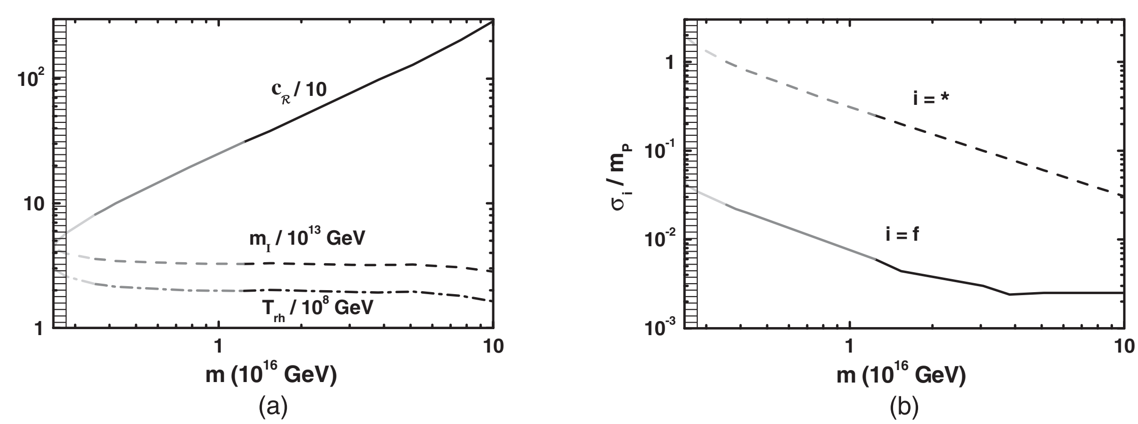


FIG. 1. The allowed by Eqs. (59), (60a), (60b), and (61b) values of $c_{\mathcal{R}}$ (solid line), $m_{\rm I}$—given by Eq. (36)—(dashed line) and $T_{\rm rh}$—given by Eq. (41)—(dot-dashed line) [$\sigma_f$ (solid line) and $\sigma_*$ (dashed line)] versus $m$ (a)[(b)] for $\lambda_1 \ll \lambda_2 = \lambda_3 = 0.5$. The light gray and gray segments denote values of the various quantities satisfying Eq. (61)a too, whereas along the light gray segments we obtain $\sigma_* \gtrsim m_{\rm P}$. Values of the parameters to the right of the lined region correspond to $n_s$'s lying within its 68% c.l. observationally favored region.

for $\hat{N}_* \simeq 54.5$. From Fig. 1(a), we observe that $m$ depends on $c_{\mathcal{R}}$ almost linearly whereas $m_{\rm I}$ remains close to $10^{13}$ GeV as we anticipated in Eqs. (33) and (36), respectively. As a result of the latter effect, $T_{\rm rh}$ given by Eq. (41) remains also almost constant. As $m$ (or $c_{\mathcal{R}}$) decreases below its maximal value in its allowed region in Eq. (70), we obtain

$$0.965 \lesssim n_{\rm s} \lesssim 0.991, \tag{71a}$$

$$6.5 \lesssim -\alpha_{\rm s}/10^{-4} \lesssim 12, \tag{71b}$$

$$3.1 \lesssim r/10^{-3} \lesssim 7.3. \tag{71c}$$

Clearly, the predicted $n_{\rm s}$, $\alpha_{\rm s}$ and $r$ can lie within the allowed ranges given in Eqs. (60b)–(60d) respectively. In particular, values of the various parameters plotted in Fig. 1, which lie to the right of the lined regions correspond to $n_{\rm s} \simeq (0.965–0.98)$. This result is consistent with the 68% c.l. observationally favored region—see Eq. (60b). It is notable, however, that $n_{\rm s}$ increases impressively for $\sigma_*/m_{\rm P} > \sqrt{6}$, contrary to the situation in models of nMCI with quadratic coupling to $\mathcal{R}$ where $n_{\rm s}$ remains constantly close to its central observational favored value in Eq. (60b)—cf. Ref. [11].

As regards the $\tilde{G}$ abundance, employing Eq. (43), we find

$$3.5 \lesssim Y_{\tilde{G}}/10^{-14} \lesssim 8.4 \tag{72}$$

as $m$ varies within its allowed range in Eq. (70). Comparing this result with the limits of Eq. (68), we infer that our model is consistent with the relevant restriction for $m_{\tilde{G}} \gtrsim (8–10)$ TeV.

### *2. The stage of nonthermal leptogenesis*

As we show above, the stage of nMCI predicts almost constant values of $m_{\rm I}$ and $T_{\rm rh}$—recall that we consider $\lambda_i$'s of the order of 0.1. In other words, the post-inflationary evolution in our setup is largely independent of the precise value of $m$ in the range of Eq. (70). As a consequence, $Y_B$ calculated by Eq. (42) does not vary with $m$, contrary to the naive expectations. Just for definiteness we take throughout this section $m = 4.2 \times 10^{15}$ GeV which corresponds to $c_{\mathcal{R}} = 100$, $n_{\rm s} = 0.969$, $m_{\rm I} = 3.4 \times 10^{13}$ GeV and $T_{\rm rh} = 2.1 \times 10^8$ GeV ($Y_{\tilde{G}} \simeq 4 \times 10^{-14}$)—recall that we use $\lambda_1 \ll \lambda_2 = \lambda_3 = 0.5$.

On the contrary, $Y_B$ in our approach depends crucially on the low-energy parameters related to the neutrino physics. In our numerical program, for a given neutrino mass scheme, we take as input parameters: $m_{l\nu}$, $\varphi_1$, $\varphi_2$ and the best-fit values of the neutrino parameters listed in paragraph 5 of Sec. VA. We then find the *renormalization group* (RG) evolved values of these parameters at the scale of nTL, $\Lambda_L$, which is taken to be $\Lambda_L = m_{\rm I}$, integrating numerically the complete expressions of the RG

TABLE IV. Parameters yielding the correct BAU for various neutrino mass schemes.

| Parameters | Cases | | | | | | |
|---|---|---|---|---|---|---|---|
| | A | B | C | D | E | F | G |
| | Normal Hierarchy | | Degenerate Masses | | | Inverted Hierarchy | |
| **Low Scale Parameters** | | | | | | | |
| $m_{1\nu}/0.1$ eV | 0.05 | 0.1 | 0.5 | 1. | 0.7 | 0.5 | 0.49 |
| $m_{2\nu}/0.1$ eV | 0.1 | 0.13 | 0.51 | 1.0 | 0.705 | 0.51 | 0.5 |
| $m_{3\nu}/0.1$ eV | 0.5 | 0.51 | 0.71 | 1.12 | 0.5 | 0.1 | 0.05 |
| $\sum_i m_{i\nu}/0.1$ eV | 0.65 | 0.74 | 1.7 | 3.1 | 1.9 | 1.1 | 1 |
| $m_\beta/0.1$ eV | $8 \times 10^{-3}$ | 0.013 | 0.19 | 0.46 | 0.3 | 0.42 | 0.44 |
| $\varphi_1$ | $\pi$ | $\pi$ | 0 | $\pi/4$ | $\pi/4$ | $\pi/4$ | $\pi/4$ |
| $\varphi_2$ | 0 | 0 | $5\pi/6$ | $\pi$ | $\pi$ | $\pi/2$ | $\pi/4$ |
| **Leptogenesis-Scale Parameters** | | | | | | | |
| $m_{1\rm D}/0.1$ GeV | 2 | 2.5 | 4 | 8 | 9 | 6 | 5 |
| $m_{2\rm D}/0.1$ GeV | 3 | 3.49 | 5 | 9.3 | 6 | 3 | 1 |
| $m_{3\rm D}/0.1$ GeV | 6.7 | 4 | 8 | 11 | 4.7 | 2 | 2.1 |
| $M_{1\nu^c}/10^{11}$ GeV | 2.5 | 2.4 | 3.3 | 6.5 | 4.6 | 1 | 0.3 |
| $M_{2\nu^c}/10^{11}$ GeV | 11 | 7.3 | 5.2 | 8.13 | 4.9 | 5.56 | 4.3 |
| $M_{3\nu^c}/10^{11}$ GeV | 17 | 7.6 | 6 | 8.36 | 8.6 | 6.7 | 5.1 |
| $\Delta_{iji}/10^4$ | 4.5 | 0.5 | 0.96 | 0.05 | 0.3 | 1.6 | 1.4 |
| $\Delta_{ijj}/10^4$ | 1.6 | 0.54 | 0.48 | 0.04 | 0.3 | 1.2 | 3.5 |
| (with $i = 2$ and $j = 3$ except for case E where $i = 1$ and $j = 2$) | | | | | | | |
| **Resulting $B$-Yield** | | | | | | | |
| $10^{11} Y_B^0$ | 8.3 | 7.4 | 6.3 | 3.3 | 7.2 | 9.3 | 4.8 |
| $10^{11} Y_B$ | 8.7 | 8.85 | 8.98 | 8.4 | 8.9 | 8.96 | 8.95 |

equations—given in Ref. [52]—for $m_{i\nu}$, $\theta_{ij}$, $\delta$, $\varphi_1$ and $\varphi_2$. In doing this, we consider the MSSM with $\tan\beta \simeq 50$ (favored by the preliminary LHC results [53]) as an effective theory between $\Lambda_L$ and a SUSY-breaking scale, $M_{\rm SUSY} = 1.5$ TeV. Below $M_{\rm SUSY}$ the running of the various parameters is realized considering the particle content of SM with a mass of about 120 GeV for the light Higgs. Following the procedure described in Sec. IV B, we evaluate $M_{i\nu^c}$ at $\Lambda_L$ taking $m_{i\rm D}$ as free parameters. In our approach we do not consider the running of $m_{i\rm D}$ and $M_{i\nu^c}$ and therefore we give their values at $\Lambda_L$.

We start the exposition of our results arranging in Table IV some representative values of the parameters leading to the correct BAU for normally hierarchical (cases A and B), degenerate (cases C, D and E) and invertedly hierarchical (cases F and G) neutrino masses. For comparison we display the $B$-yield with ($Y_B$) or without ($Y_B^0$) taking into account the RG effects. We observe that the two results differ appreciably especially in the cases with degenerate or IO $m_{i\nu}$'s. As it is evident from the $m_{i\rm D}$'s chosen, our model is not compatible with any GUT-inspired pattern of large hierarchy between the $m_{i\rm D}$'s. In particular, we need $m_{1\rm D} < m_{2\rm D} < m_{3\rm D}$ [$m_{3\rm D} < m_{2\rm D} < m_{1\rm D}$] for NO [IO] $m_{i\nu}$'s (cases A, B, C and D [cases E, F and G]).

From Table IV we also notice that the achievement of $Y_B$ within the range of Eq. (67) dictates mostly proximity between two of the $M_{i\nu^c}$'s. Indeed, except for the case A, we obtain $M_{2\nu^c}/M_{1\nu^c} \simeq 1.06$ in case E and $M_{3\nu^c}/M_{2\nu^c} < 1.2$ in the residual cases. However, it is clear from the displayed $\Delta_{iji}$'s and $\Delta_{iji}$'s (with $i = 2$ and $j = 3$ for all the cases besides case E where $i = 1$ and $j = 2$) that in our framework the conditions of Eq. (45) are comfortably retained and therefore, our proposal is crucially different from that of resonant leptogenesis [44–46]—it rather resembles that of Ref. [28]. On the other hand, the correctness of $Y_B$ in the case A entails $M_{2\nu^c}$ and $M_{3\nu^c}$ [$\lambda_{2\nu^c}$ and $\lambda_{3\nu^c}$] roughly larger than $10^{12}$ GeV [unity]. In all cases the current limit of Eq. (65) is safely met—the case D approaches it—, while $m_\beta$ turns out to be well below the projected sensitivity of KATRIN [51].

To highlight further our conclusions inferred from Table IV, we can fix $m_{l\nu}$ ($m_{1\nu}$ for NO $m_{i\nu}$'s or $m_{3\nu}$ for IO $m_{i\nu}$'s) $m_{1\rm D}$, $\varphi_1$ and $\varphi_2$ to their values shown in this table and vary $m_{2\rm D}$ and $m_{3\rm D}$ so that the central value of Eq. (67) is achieved. The resulting contours in the $m_{2\rm D} - m_{3\rm D}$ plane are presented in Fig. 2(a)—since the range of Eq. (67) is very narrow the possible variation of the drawn lines is negligible. The resulting values of $M_{j\nu^c}$

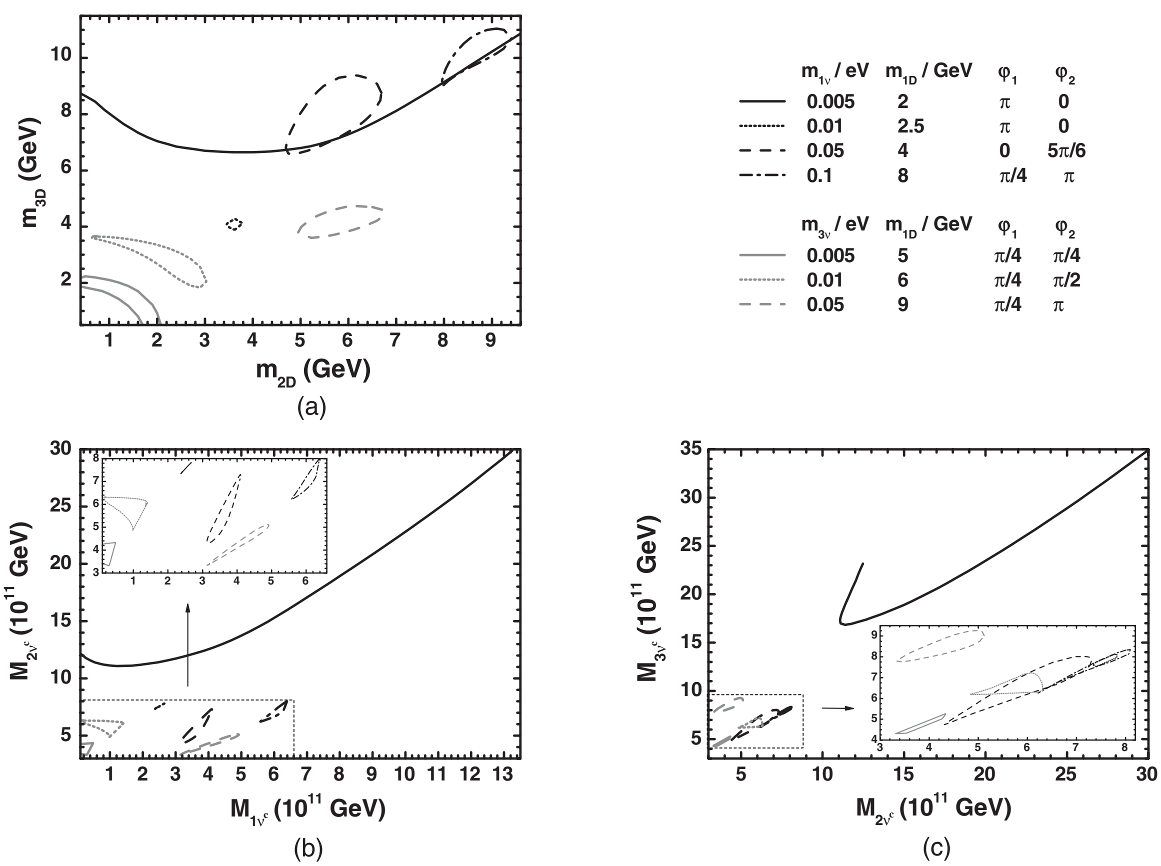


FIG. 2. Contours in the $m_{2\rm D} - m_{3\rm D}$ (a) $M_{1\nu^c} - M_{2\nu^c}$ (b) and $M_{2\nu^c} - M_{3\nu^c}$ (c) plane yielding the central $Y_B$ in Eq. (67), for various ($m_{\ell\nu}$, $m_{1\rm D}$, $\varphi_1$, $\varphi_2$)'s indicated next to the graph (a) and NO [IO] $m_{i\nu}$'s (black [gray] lines).

are displayed in $M_{1\nu^c} - M_{2\nu^c}$ and $M_{2\nu^c} - M_{3\nu^c}$ plane—see Fig. 2(b) and 2(c) respectively. The conventions adopted for the types and the color of the various lines are also described next to the graphs (a) of Fig. 2. In particular, we use black [gray] lines for NO [IO] $m_{i\nu}$'s. Besides the case with $m_{1\nu} = 0.005$ eV we observe that every curve in all graphs has two branches and not large hierarchies allowed in the sectors of both the $m_{\rm D}$'s and $M_{\nu^c}$'s. Note that the black contour for $m_{1\nu} = 0.01$ eV in Fig. 2(c) is included within the one for $m_{1\nu} = 0.1$ eV and so, it is not quite distinguishable. For $m_{1\nu} = 0.005$ eV, $\lambda_{3\nu^c}$ saturates the perturbation limit. Since we expect that the $\lambda_{i\nu^c}$'s increase [54] due to their RG running from low to higher scale, our results do not jeopardize the validity of the conventional perturbation approach up to the scale $\Lambda_L$. In all cases we find that $m_{i\rm D} \lesssim 10$ GeV.

It is worth emphasizing that, although our mechanism of nTL is connected with the specific inflationary model under consideration, it can have a much wider applicability. It can be realized within other models of inflation with similar inflaton mass and reheat temperature, since it is largely independent of the details of the inflationary phase but restricts mainly the yet unknown parameters of neutrino physics ($m_{i\nu}$, $m_{i\rm D}$, $\varphi_1$, $\varphi_2$).

## VI. CONCLUSIONS

We investigated a novel inflationary scenario in which the inflaton field appears in a bilinear superpotential term and in a linear holomorphic function included in a logarithmic Kähler potential. The latter function can be interpreted in JF as a nonminimal coupling to gravity, whose the strength is constrained so as the EF inflationary potential can be flattened enough to support a stage of nonminimal inflation compatible with observations. The inflationary model was embedded in a moderate extension of MSSM augmented by three RH neutrino superfields and three other singlet superfields, which lead to a PQPT tied to renormalizable superpotential terms. The PQPT follows nMCI and resolves the strong $CP$ and the $\mu$ problems of MSSM and also provides RH neutrinos with masses lower than about $10^{12}$ GeV. The possible catastrophic production of domain walls can be eluded by the introduction of extra matter superfields which can be chosen so that the MSSM gauge coupling constant unification is not disturbed. For $\tilde{G}$ masses larger than 8 TeV, observationally safe reheating of the universe with $T_{\rm rh} \simeq 10^8$ GeV can be accomplished by a three-body decay of the inflaton. The subsequent out-of-equilibrium decays of the produced RH sneutrinos can generate the required by the observations BAU consistently with the present low-energy neutrino data, provided that the Dirac neutrino masses are constrained in the range 1–10 GeV for all the light-neutrino mass schemes. It is gratifying that the degeneracy of the masses of the RH (s) neutrinos required by the mechanism of nTL in our model is low enough compared with their decay widths, so that perturbative calculation remains safely valid. Finally, we briefly discussed scenaria in which the potential axino and saxion overproduction problems can be avoided.

## ACKNOWLEDGMENTS

C. P. acknowledges the Bartol Research Institute and the Department of Physics and Astronomy of the University of Delaware for its warm hospitality, during which this work has been initiated. Q. S. acknowledges support by the DOE Grant No. DE-FG02-12ER41808. We would like to thank G. Lazarides, H. M. Lee, W.-I. Park, M. Ur Rehman and N. Toumbas for helpful discussions.

---


[1] K. Nozari and S. D. Sadatian, Mod. Phys. Lett. A **23**, 2933 (2008); K. Nozari and S. Shafizadeh, Phys. Scr. **82**, 015901 (2010).

[2] J. L. Cervantes-Cota and H. Dehnen, Nucl. Phys. **B442**, 391 (1995); F. L. Bezrukov and M. Shaposhnikov, Phys. Lett. B **659**, 703 (2008); A. Barvinsky *et al.*, J. Cosmol. Astropart. Phys. 11 (2008) 021; A. De Simone, M. P. Hertzberg, and F. Wilczek, Phys. Lett. B **678**, 1 (2009).

[3] R. Fakir and W. G. Unruh, Phys. Rev. D **41**, 1783 (1990); E. Komatsu and T. Futamase, Phys. Rev. D **59**, 064029 (1999); S. Tsujikawa and B. Gumjudpai, Phys. Rev. D **69**, 123523 (2004).

[4] T. E. Clark, B. Liu, S. T. Love, and T. ter Veldhuis, Phys. Rev. D **80**, 075019 (2009); R. N. Lerner and J. McDonald, Phys. Rev. D **80**, 123507 (2009).

[5] R. N. Lerner and J. McDonald, Phys. Rev. D **82**, 103525 (2010); G. F. Giudice and H. M. Lee, Phys. Lett. B **694**, 294 (2011); F. Bauer and D. A. Demir, Phys. Lett. B **698**, 425 (2011).

[6] S. C. Park and S. Yamaguchi, J. Cosmol. Astropart. Phys. 08 (2008) 009; S. Koh and M. Minamitsuji, Phys. Rev. D **83**, 046009 (2011); A. De Felice, S. Tsujikawa, J. Elliston, and R. Tavakol, J. Cosmol. Astropart. Phys. 08 (2011) 021.

[7] C. Pallis, Phys. Lett. B **692**, 287 (2010).

[8] N. Okada, M. U. Rehman, and Q. Shafi, Phys. Rev. D **82**, 043502 (2010); Phys. Lett. B **701**, 520 (2011).

[9] M. B. Einhorn and D. R. T. Jones, J. High Energy Phys. 03 (2010) 026; S. Ferrara, R. Kallosh, A. Linde, A. Marrani, and A. Van Proeyen, *et al.*, Phys. Rev. D **82**, 045003 (2010); H. M. Lee, J. Cosmol. Astropart. Phys. 08 (2010) 003; S. Ferrara *et al.*, Phys. Rev. D **83**, 025008 (2011).

[10] R. Kallosh and A. Linde, J. Cosmol. Astropart. Phys. 11 (2010) 011; A. Linde, M. Noorbala, and A. Westphal, J. Cosmol. Astropart. Phys. 03 (2011) 013.

[11] C. Pallis and N. Toumbas, J. Cosmol. Astropart. Phys. 02 (2011) 019.

[12] C. Pallis and N. Toumbas, J. Cosmol. Astropart. Phys. 12 (2011) 002.

[13] Y.G. Kim, H.M. Lee, and W.-I. Park, J. High Energy Phys. 08 (2011) 126; M. Arai, S. Kawai, and N. Okada, Phys. Rev. D **84**, 123515 (2011); arXiv:1112.2391.

[14] M. Kawasaki, M. Yamaguchi, and T. Yanagida, Phys. Rev. Lett. **85**, 3572 (2000); Phys. Rev. D **63**, 103514 (2001); S. Antusch, M. Bastero-Gil, K. Dutta, S.F. King, and P.M. Kostka, Phys. Lett. B **679**, 428 (2009); F. Takahashi, Phys. Lett. B **693**, 140 (2010).

[15] P. Brax and J. Martin, Phys. Rev. D **72**, 023518 (2005); I. Ben-Dayan and M.B. Einhorn, J. Cosmol. Astropart. Phys. 12 (2010) 002; K. Nakayama and F. Takahashi, J. Cosmol. Astropart. Phys. 02 (2011) 010.

[16] E. Komatsu *et al.* (WMAP Collaboration), Astrophys. J. Suppl. Ser. **192**, 18 (2011); http://lambda.gsfc.nasa.gov/product/map/dr2/parameters.cfm.

[17] R. Peccei and H. Quinn, Phys. Rev. Lett. **38**, 1440 (1977); S. Weinberg, *ibid.* **40**, 223 (1978); F. Wilczek, *ibid.* **40**, 279 (1978).

[18] H. Baer, A.D. Box, and H. Summy, J. High Energy Phys. 10 (2010) 023; H. Baer, A. Lessa, and W. Sreethawong, J. Cosmol. Astropart. Phys. 01 (2012) 036.

[19] M. Kawasaki, N. Kitajima, and K. Nakayama, Phys. Rev. D **83**, 123521 (2011); E.J. Chun, Phys. Rev. D **84**, 043509 (2011); K.-Y. Choi, L. Covi, J.E. Kim, and L. Roszkowski, J. High Energy Phys. 04 (2012) 106; K.J. Bae, E.J. Chun, and S.H. Im, J. Cosmol. Astropart. Phys. 03 (2012) 013.

[20] J.E. Kim, Phys. Lett. B **136**, 378 (1984); J.E. Kim and H.P. Nilles, Phys. Lett. B **138**, 150 (1984); T. Goto and M. Yamaguchi, Phys. Lett. B **276**, 103 (1992).

[21] P. Minkowski, Phys. Lett. B **67**, 421 (1977); T. Yanagida, *Proceedings of the Workshop on the Unified Theory and the Baryon Number in the Universe*, edited by O. Sawada and A. Sugamoto (KEK, Tsukuba, Japan, 1979), p. 95; M. Gell-Mann, P. Ramond, and R. Slansky, *Supergravity*, edited by P. van Nieuwenhuizen *et al.* (North Holland, Amsterdam, 1979), p. 315; S.L. Glashow, *Proceedings of the 1979 Cargese Summer Institute on Quarks and Leptons*, edited by M. Levy *et al.* (Plenum Press, New York, 1980), p. 687; R.N. Mohapatra and G. Senjanovíc, Phys. Rev. Lett. **44**, 912 (1980).

[22] P. Sikivie, Phys. Rev. Lett. **48**, 1156 (1982).

[23] G. Lazarides and Q. Shafi, Phys. Lett. B **115**, 21 (1982); H. Georgi and M.B. Wise, *ibid.* **116**, 123 (1982).

[24] G. Lazarides and Q. Shafi, Phys. Lett. B **489**, 194 (2000); G. Lazarides and C. Pallis, Phys. Rev. D **82**, 063535 (2010).

[25] G. Lazarides and Q. Shafi, Phys. Lett. B **258**, 305 (1991); K. Kumekawa, T. Moroi, and T. Yanagida, Prog. Theor. Phys. **92**, 437 (1994); G. Lazarides, R.K. Schaefer, and Q. Shafi, Phys. Rev. D **56**, 1324 (1997); G. Lazarides, arXiv:hep-ph/9905450.

[26] T. Schwetz, M. Tortola, and J.W.F. Valle, New J. Phys. **13**, 109401 (2011).

[27] G.L. Fogli, E. Lisi, A. Marrone, A. Palazzo, and A.M. Rotunno, Phys. Rev. D **84**, 053007 (2011).

[28] T. Asaka, K. Hamaguchi, M. Kawasaki, and T. Yanagida, Phys. Rev. D **61**, 083512 (2000); M. Fujii, K. Hamaguchi, and T. Yanagida, Phys. Rev. D **65**, 115012 (2002).

[29] M. Yu. Khlopov and A.D. Linde, Phys. Lett. B **138**, 265 (1984); J. Ellis, J.E. Kim, and D.V. Nanopoulos, Phys. Lett. B **145**, 181 (1984).

[30] M. Bolz, A. Brandenburg, and W. Buchmüller, Nucl. Phys. B **606**, 518 (2001); **790**, 336(E) (2008); J. Pradler and F.D. Steffen, Phys. Rev. D **75**, 023509 (2007).

[31] M. Kawasaki, K. Kohri, and T. Moroi, Phys. Lett. B **625**, 7 (2005); Phys. Rev. D **71**, 083502 (2005); R.H. Cyburt *et al.*, Phys. Rev. D **67**, 103521 (2003); J.R. Ellis, K.A. Olive, and E. Vangioni, Phys. Lett. B **619**, 30 (2005).

[32] See e.g. M. Peskin, arXiv:0801.1928.

[33] S.R. Coleman and E.J. Weinberg, Phys. Rev. D **7**, 1888 (1973).

[34] D.H. Lyth and A. Riotto, Phys. Rep. **314**, 1 (1999); A. Mazumdar and J. Rocher, Phys. Rep. **497**, 85 (2011).

[35] D.S. Salopek, J.R. Bond, and J.M. Bardeen, Phys. Rev. D **40**, 1753 (1989); F. Bauer and D.A. Demir, Phys. Lett. B **665**, 222 (2008); N. Makino and M. Sasaki, Prog. Theor. Phys. **86**, 103 (1991); R. Fakir, S. Habib, and W. Unruh, Astrophys. J. **394**, 396 (1992); D.I. Kaiser, Phys. Rev. D **52**, 4295 (1995); T. Chiba and M. Yamaguchi, J. Cosmol. Astropart. Phys. 10 (2008) 021.

[36] L. Kofman, A.D. Linde, and A.A. Starobinsky, Phys. Rev. Lett. **73**, 3195 (1994); Phys. Rev. D **56**, 3258 (1997).

[37] J. Garcia-Bellido, D.G. Figueroa, and J. Rubio, Phys. Rev. D **79**, 063531 (2009); F. Bezrukov, D. Gorbunov, and M. Shaposhnikov, J. Cosmol. Astropart. Phys. 06 (2009) 029.

[38] G.N. Felder, L. Kofman, and A.D. Linde, Phys. Rev. D **59**, 123523 (1999).

[39] C. Pallis, Nucl. Phys. **B751**, 129 (2006).

[40] K. Hamaguchi, Ph.D. thesis, arXiv:hep-ph/0212305; W. Buchmuller, R.D. Peccei, and T. Yanagida, Annu. Rev. Nucl. Part. Sci. **55**, 311 (2005).

[41] M. Endo, M. Kawasaki, F. Takahashi, and T.T. Yanagida, Phys. Lett. B **642**, 518 (2006); M. Endo, F. Takahashi, and T.T. Yanagida, Phys. Rev. D **76**, 083509 (2007).

[42] H. Baer, S. Kraml, A. Lessa, and S. Sekmen, J. Cosmol. Astropart. Phys. 04 (2011) 039.

[43] M. Kawasaki, K. Nakayama, and M. Senami, J. Cosmol. Astropart. Phys. 03 (2008) 009.

[44] M. Flanz, E.A. Paschos, and U. Sarkar, Phys. Lett. B **345**, 248 (1995); **382**, 447(E) (1996); M. Flanz, E.A. Paschos, U. Sarkar, and J. Weiss, Phys. Lett. B **389**, 693 (1996); L. Covi, E. Roulet, and F. Vissani, Phys. Lett. B **384**, 169 (1996).

[45] A. Pilaftsis, Phys. Rev. D **56**, 5431 (1997); A. Pilaftsis and T.E.J. Underwood, Nucl. Phys. **B692**, 303 (2004); F.F. Deppisch and A. Pilaftsis, Phys. Rev. D **83**, 076007 (2011).

[46] W. Buchmuler and M. Plumacher, Phys. Lett. B **431**, 354 (1998); A. Anisimov, A. Broncano, and M. Plu-macher, Nucl. Phys. **B737**, 176 (2006); M. Garny, A. Hohenegger, A. Kartavtsev, and M. Lindner, Phys. Rev. D **81**, 085027 (2010).

[47] G.C. Branco, R. Gonzalez Felipe, F.R. Joaquim, and M.N. Rebelo, Nucl. Phys. **B640**, 202 (2002); E.K. Akhmedov, M. Frigerio, and A.Y. Smirnov, J. High Energy Phys. 09 (2003) 021; S. Pascoli, S.T. Petcov, and W. Rodejohann, Phys. Rev. D **68**, 093007 (2003); V.N. Şenoğuz, Phys. Rev. D **76**, 013005 (2007).

[48] J. Kopp, Int. J. Mod. Phys. C **19**, 523 (2008).
[49] C. P. Burgess, H. M. Lee, and M. Trott, J. High Energy Phys. 09 (2009) 103; J. L. F. Barbon and J. R. Espinosa, Phys. Rev. D **79**, 081302 (2009); C. P. Burgess, H. M. Lee, and M. Trott, J. High Energy Phys. 07 (2010) 007; R. N. Lerner and J. McDonald, J. Cosmol. Astropart. Phys. 04 (2010) 015; M. P. Hertzberg, J. High Energy Phys. 11 (2010) 023; F. Bezrukov *et al.*, J. High Energy Phys. 01 (2011) 016; M. Atkins and X. Calmet, Phys. Lett. B **697**, 37 (2011).
[50] H. V. Klapdor-Kleingrothaus *et al.*, Eur. Phys. J. A **12**, 147 (2001); C. E. Aalseth *et al.* (IGEX Collaboration), Phys. Rev. D **65**, 092007 (2002); J. Bonn *et al.*, Nucl. Phys. B, Proc. Suppl. **91**, 273 (2001); V. M. Lobashev *et al.*, Nucl. Phys. B, Proc. Suppl. **91**, 280 (2001).
[51] A. Osipowicz *et al.* (KATRIN Collaboration), arXiv:hep-ex/0109033.
[52] S. Antusch, J. Kersten, M. Lindner, and M. Ratz, Nucl. Phys. **B674**, 401 (2003); http://www.ph.tum.de/~mratz/AnalyticFormulae.
[53] A. Arbey *et al.*, Phys. Lett. B **708**, 162 (2012); M. Kadastik, K. Kannike, A. Racioppi, and M. Raidal, J. High Energy Phys. 05 (2012) 061; I. Gogoladze, Q. Shafi, and C. S. Un, arXiv:1112.2206; O. Buchmueller *et al.*, arXiv:1112.3564; N. Karagiannakis, G. Lazarides, and C. Pallis, arXiv:1201.2111.
[54] H. Murayama, H. Suzuki, and T. Yanagida, Phys. Lett. B **291**, 418 (1992); K. Choi, E. J. Chun, and J. E. Kim, Phys. Lett. B **403**, 209 (1997); W. I. Park, J. High Energy Phys. 07 (2010) 085.